Nature of short, high-amplitude compressive stress pulses in a periodic dissipative laminate

Pedro Franco Navarro,[1] David J. Benson,[2] and Vitali F. Nesterenko[1,3]
[1]*Department of Mechanical and Aerospace Engineering, University of California, San Diego, La Jolla, California 92093-0411, USA*
[2]*Department of Structural Engineering, University of California, San Diego, La Jolla, California 92093-0085, USA*
[3]*Materials Science and Engineering Program, University of California, San Diego, La Jolla, California 92093-0418, USA*
(Received 5 June 2015; published 18 December 2015)

We study the evolution of high-amplitude stress pulses in periodic dissipative laminates taking into account the nonlinear constitutive equations of the components and their dissipative behavior. Aluminum-tungsten laminate was selected due to the large difference in acoustic impedances of components, the significant nonlinearity of the aluminum constitutive equation at the investigated range of stresses, and its possible practical applications. Laminates with different cell size, which controls the internal time scale, impacted by plates with different thicknesses that determine the incoming pulse duration, were investigated. It has been observed that the ratio of the duration of the incoming pulse to the internal characteristic time determines the nature of the high-amplitude dissipative propagating waves—a triangular oscillatory shock–like profile, a train of localized pulses, or a single localized pulse. These localized quasistationary waves resemble solitary waves even in the presence of dissipation: The similar pulses emerged from different initial conditions, indicating that they are inherent properties of the corresponding laminates; their characteristic length scale is determined by the scale of mesostructure, nonlinear properties of materials, and the stress amplitude; and a linear relationship exists between their speed and amplitude. They mostly recover their shapes after collision with phase shift. A theoretical description approximating the shape, length scale, and speed of these high-amplitude dissipative pulses was proposed based on the Korteweg–de Vries equation with a dispersive term determined by the mesostructure and a nonlinear term derived using Hugoniot curves of components.

DOI: 10.1103/PhysRevE.92.062917 PACS number(s): 05.45.Yv, 46.40.Cd

I. INTRODUCTION

The response of materials to high-amplitude shock wave loading is usually analyzed based on the assumption that the shock wave has reached a steady state which is assumed to happen when the shock wave propagates a distance of a few shock front widths [1]. This assumption allows the use of the conservation laws across the shock front, resulting in the Rankine-Hugoniot equations connecting the states in front of and behind the stationary shock wave, if the duration of the pulse is long enough [1–3].

The case of laminated materials presents a challenge for such an approach, and the first studies to characterize the behavior of these materials in the acoustic realm, including their dispersive properties due to periodic mesostructure, can be found in [4–6]. For example, in [6] the authors propose a one-dimensional lattice model that includes geometrical dispersion. Their model agrees with the results of ultrasonic experiments. The behavior of an Al-W composite (W fibers placed in Al matrix) under impact by a thick Al plate, generating a semi-infinite loading pulse to avoid the formation of release waves on the back of the flyer plate, was investigated in [7]. The experimental results related to shock rise time show good agreement with the numerical modeling based on the lattice model and nonlinear elastic-plastic response. The structuring of the wave front occurred near the impact surface. The formation of a steady shock wave profile in laminate materials can require much longer distances because the establishment of steady state behind shock can be delayed due to the longer mechanical and thermal relaxation processes. This is clearly illustrated in periodic systems composed from metal or glass plates with gaps between them where establishment of the steady state behind the shock wave happened after about ten reverberations of waves behind the leading part of the pulse [8,9]. In the case when laminate materials are loaded by a long duration incoming disturbance (especially for small size of the cell in laminate material) the stationary shock wave can be formed and the final state can still be described in the frame of Hugoniot approach if conditions of thermal and mechanical equilibrium hold. In this case the Hugoniot curve is not sensitive to the mesostructural properties of material, e.g., cell size.

In some applications laminates are subjected to very short duration loading pulses, created, for example, by powerful lasers. But in the case of the short incoming pulse, caused by impact of a thin plate with thickness comparable to the thickness of a cell in the laminate or contact explosion of a thin layer of explosive [9], or by laser excitation [10,11], the stationary shock wave is not formed in the laminate. In this case the Hugoniot curve does not describe the states of dynamically compressed components and their response can be very sensitive to the pulse length and material mesostructure. For example, at short duration of incoming pulse interesting phenomena such as anomalous dependence of leading shock amplitude on the cell size (increase of amplitude with decrease of cell size) were observed in experiments and in numerical calculations [9,12–14], being in contradiction with behavior expected from acoustic approximation [15]. Nonlinearity in the stress-strain relation was responsible for these deviations from linear elastic behavior.

In the case of relatively short duration of loading pulse a combination of dispersive properties and nonlinearity in layered media give rise to a qualitatively new, solitarylike pulses numerically investigated in [16–22].

The paper [16] considers the evolution of nonlinear elastic waves in a nondissipative layered media excited by the

motion of the boundary and explores the effects of impedance mismatch between layers, which is a cause for a dispersion. They observed numerically that at the investigated boundary conditions the impedance mismatch coupled with the nonlinearities, introduced by nonlinear stress-strain dependence of components, resulted in a transformation of an incoming pulse into a train of localized pulses. The authors called them *stegotons* since it was not clear whether these localized pulse were formally solitons. They noticed that the width of each stegoton is about ten layers and it is independent of the size of the layers, but it depends on the wave amplitude. Their speed was equal to the effective sound speed for the linearized medium plus a term linearly depending on the amplitude. Their shape was roughly approximated by the sech^2 function of time; both properties are characteristic for the Korteweg–de Vries (KdV) solitons. Two stegotons with different amplitudes were excited at the boundary and the stegoton with the higher amplitude travels faster and eventually overtakes the first one with a smaller amplitude. As in the case of an interacting solitary wave the colliding stegotons roughly assumed their initial shape after separation with some phase shift.

In [16] the authors considered a comparison between a nonlinear laminate material with one of the layers having very small density and bulk elastic modulus (ratio of densities being equal to 10^{-3} and ratio of bulk moduli being equal to 2.5×10^{-4}) with the Toda lattice where particles of similar masses alternate with springs. They selected the unit cell in the Toda lattice being equal to the unit cell of the laminate (composed from the two different layers) and masses of particles being equal to the average density of the layered medium. The force in effective springs had exponential dependence on the strain mimicking force in the Toda lattice with the coefficient in exponent related to the smallest bulk modulus. This interaction force resulted in a correct effective sound speed in a linearized medium. In this special limited choice of parameters of laminate material the authors found that solitarylike behavior of laminate can be modeled directly by the Toda lattice. The authors also introduce a set of homogenized equations which support the solitarylike solutions similar to the direct solutions of the original hyperbolic system.

The paper [17] emphasized that the microstructure of materials characterized by intrinsic space scales, e.g., lattice period, size of crystalline grain, thickness of layers in laminates, and distance between microcracks, is responsible for the effects of dispersion and being combined with nonlinear behavior results in phenomena like solitons. The authors considered a discrete and continuum approach for the modeling of the effects of microstructure and nonlinearity following the Mindlin analysis [18]. Depending on the initial and boundary conditions they demonstrated formation of a single solitarylike pulse or a train of these pulses. They obtained good agreement with experimental data [19] of the stress history in the laminate polycarbonate (layer thickness 0.39 mm)–stainless steel (0.19 mm) at the distance 3.44 mm from the impacted face using a finite-volume algorithm and nonlinear parameter only for the polycarbonate. The simplified boundary conditions in calculations modeling plate impact in experiments, were given by a step function with the velocity amplitude equal to the velocity of the impacted plate (1043 m/s) with thickness 2.87 mm. However, the amplitude of the particle velocity in experiments on the interface with the laminate (having polycarbonate as the first layer) and polycarbonate impactor with velocity 1043 m/s should be equal to half of this value—521.5 m/s. Also it is not clear what duration was selected of the used step function (the authors probably used a rectangular function) as a boundary conditions modeling impact by a plate with finite thickness, which was able to provide a good fit to experimental data.

The propagation and head-on collisions of localized initial pulses were numerically investigated in [20] for microstructural materials with different values of microscale nonlinearity parameter. It was found that the interaction between localized waves is not completely elastic. The phase shift observed in such interactions is increased when the amplitudes are dissimilar and with a longer observation time. Over short time intervals and small number of collisions the behavior of these localized pulses was close to the solitonic behavior in all considered cases.

The emergence of two solitary trains from the localized initial condition was numerically investigated using a Boussinesq-type equation [21] for nonlinear microstructured solids also following the Mindlin approach [18]. On the long time scale they observed establishment of the stationary amplitudes of each emerging localized pulse in the train with linear dependence of their speed on the amplitude. The speed and amplitudes of localized pulses were traced after their multiple collisions. They display the main characteristics of classical solitons though their interaction is not fully elastic, especially at the low amplitudes. Thus the authors suggested using the term "quasisolitons" to distinguish them from "pure solitons" characteristic for highly idealized nonlinear dispersive systems.

The propagation of nonlinear longitudinal strain waves in the case of uniaxial strain state in a layered material was studied using a macroscopic Boussinesq-type wave equation that has been derived in a long wave approximation through a high-order asymptotic homogenization method [22]. The derived coefficients in this equation are related to the linear and nonlinear elastic moduli, densities, and volume fractions of the components. The dispersion relation in the linearized Boussinesq-type wave equation was close to the exact dispersion relation obtained using the Floquet-Bloch approach for two laminate materials (a low-contrast steel-aluminium laminate and a high-contrast laminate of steel and carbon-filled epoxy) at a ratio of cell size to characteristic wavelength less than 0.4; better agreement was obtained for high-contrast laminate. The authors also obtained the speed and width of the localized supersonic bell-shaped compression solitary wave as functions of nonlinear properties of materials and the amplitude of the solitary wave. In the case of physically linear elastic materials the geometric nonlinearity in combination with dispersion support only tension solitary waves.

The authors of [22] numerically investigated the nonstationary dynamic processes integrating macroscopic Boussinesq-type wave equation focusing on the evolution of nonlinear waves caused by different initial excitations. The initial conditions were taken as a rectangular profile with different nondimensional width δ. In case of a relatively narrow pulse of compression ($\delta = 5$) the nonlinear excitation with given amplitude resulted in two solitary waves propagating symmetrically in opposite directions with a scattering backward radiation. It is

important that at given parameters of laminates and amplitudes of excitation the formation of steady-shape solitary waves required a spatial interval three orders of magnitude larger than the cell size. A wider pulse of initial compression ($\delta = 20$) with the same amplitude resulted in a train of four solitary waves with noticeable amplitudes. The properties of these solitary waves emerging from the initial conditions were similar to the stationary solitary wave solutions of the Boussinesq-type wave equation. The narrow pulse of tension ($\delta = 5$) with the same amplitude did not evolve into a steady-shape wave producing instead a delocalization of the initial excitation.

In this paper we investigate the nature of relatively short pulses in the laminate Al-W (with the cell size equal to 1, 2, and 4 mm) generated by impact of 8- and 2-mm impactors with velocity 2800 m/s, which created realistic initial and boundary conditions reproducible in physical experiments such as loading by short and powerful lasers [10,11], contact explosion [12,13], or impacts that could be expected from space debris. The dynamic response of materials at this level of stresses is characterized by significant viscoplastic dissipation which was not considered in the previous papers related to the propagation of solitarylike pulses (stegotons) in laminates [16–22]. The dissipation can suppress the formation of these solitarylike pulses because the disturbance must travel a relatively long distance from the point of excitation before this localized pulse is formed; e.g., in [22] the formation of steady-shape solitarylike waves in a nondissipative laminate required a spatial interval three orders of magnitude larger than cell size.

We investigated the characteristic length traveled by the pulses when single solitarylike pulses (or their trains) were formed under realistic, experimentally reproducible plate impact conditions (at various thicknesses of impactor) and their subsequent rate of attenuation in the presence of dissipation.

We also investigated the head-on collisions of solitarylike pulses impacting laminates from both sides. It was proven that after interaction the most prominent change is a phase shift which agrees with the expected behavior of solitarylike waves.

We introduce a phenomenological model combining the dispersive properties of laminates, due to their periodic structure, and physical nonlinear properties of materials based on their shock adiabat (Hugoniot) instead of using third order elastic constants as in [22]. The Hugoniot curve is representing inherent nonlinear behavior of materials in a stationary shock wave at a very broad range of pressures. The combination of dispersive and nonlinear properties resulted in a KdV solitary wave. Based on this approach equations relating speed and widths of these solitarylike pulses to the geometrical and physical properties of materials in laminates were presented. The shape of the KdV solitary wave provided satisfactory fit to the shape of the localized pulses observed in numerical calculations. The speeds of KdV solitary waves also were close to the speed of localized pulses in the laminate at similar maximum pressures.

II. SIMULATIONS

We apply LS-DYNA's simulations to analyze propagation of high-amplitude dissipative nonlinear waves generated by plate impact in a one-dimensional (1D) laminate material. LS-DYNA is a general purpose finite-element software [23]; its main strength is the capability to solve highly nonlinear transient dynamic problems by explicit integration. Figure 1 represents the geometry used in our numerical modeling, where L_c is the total length of the laminate composite, L_i is the length of the impactor, and a and b are the respective thicknesses of the aluminum (Al) and tungsten (W) layers in the periodic composite material. In this paper, all layers have the same thickness ($a = b$). For the purposes of this study we selected $L_c = 280$ mm for all cases. The duration of the incoming pulses was determined by the thickness of the impactor equal to 2 and 8 mm to produce stress waves with different durations and to investigate their properties.

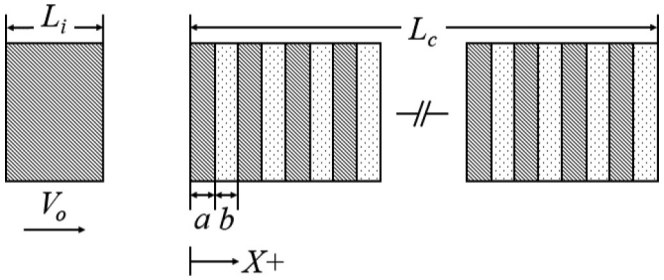

FIG. 1. Geometry of the laminate.

The impactor in the current study was an aluminum plate having high initial velocity of 2800 m/s in the $X+$ direction. In all cases, the layers of the laminate are perfectly bonded and the end of the composite is free. It is expected that the bonding between layers does not affect the compression stress wave structure and the properties of the final state behind them because we are considering only compression waves similar to [12–14].

The material model used to characterize the behavior is the well-known Steinberg-Guinan model [24,25] coupled with the Grüneisen's equation of state; this rate independent model is described as follows:

$$G = G_0\left[1 + AP\eta^{-1/3} - B\left(\frac{E - E_c}{C_p} - 300\right)\right], \quad (1)$$

where G and G_0 are current and initial shear moduli, P is the pressure, $\eta = V_0/V$, V and V_0 are current and initial specific volumes, A is a coefficient in the pressure dependence of the shear modulus, B is the coefficient in the temperature dependence of the shear modulus, and E is the total internal energy per unit volume. The cold energy of the system per unit volume E_c is defined as

$$E_c = \int_{V_0}^{V} P\,dV - 300\,C_p \exp\left\{a\left(1 - \frac{1}{\eta}\right)\right\}\eta^{\gamma_0 - a}, \quad (2)$$

where the integral in the first term is along the 300 K adiabat [24].

The melting energy (in the code it is used to check if material reached the melting conditions during the dynamic deformation) is defined as

$$E_m = E_c + C_p T_m, \quad (3)$$

TABLE I. Material properties.

Parameters	Aluminum	Tungsten
G_0(GPa)	27.6	160
Y_0(GPa)	0.29	2.2
Y_{max}(GPa)	0.76	4
β	125	24
N	0.1	0.19
A(GPa^{-1})	652	9380
B(K^{-1})	6.16×10^{-4}	1.38×10^{-4}
T_{m0}(K)	1220	4520
C_p(J/kg K)	287.67	43
γ_0	1.97	1.67
a	1.5	1.3
ρ_0(kg/m^3)	2785	19300
C_0(m/s)	5328	4030
S_1	1.338	1.237

The dependence of melting temperature T_m on specific volume based on a modified Lindemann law is expressed as

$$T_m = T_{m0} \exp\left\{2a\left(1 - \frac{1}{\eta}\right)\right\}\eta^{2(\gamma_0 - a - 1/3)}, \quad (4)$$

where γ_0 is the original Grüneisen gamma, and a is the coefficient of the volume dependence of the Grüneisen's gamma.

The yield strength (Y) of the material including dependence on pressure and effects of strain hardening and thermal softening is given by

$$Y = \frac{Y_0}{G_0}[1 + \beta(\epsilon_i + \epsilon_p)]^n \times\left[1 + AP\eta^{-1/3} - B\left(\frac{E - E_c}{C_p} - 300\right)\right], \quad (5)$$

where

$$Y_0[1 + \beta(\epsilon_i + \epsilon_p)]^n \leqslant Y_{\max}. \quad (6)$$

In Eq. (5) Y_0 is the initial yield strength and Y_{max} is the value of saturated yield strength, ϵ_i is the initial plastic strain, ϵ_p is the equivalent plastic strain added under dynamic loading, and β and n are work-hardening parameters.

Based on the Grüneisen's equation of state the pressure can be expressed as

$$P = \frac{\rho_0 C_0^2 \mu\left[1 + \left(1 - \frac{\gamma_0}{2}\right)\mu\right]}{1 - (S_1 - 1)\mu} + \gamma_0 E, \quad (7)$$

$$\mu = \frac{\rho}{\rho_0} - 1, \quad (8)$$

where ρ_0, ρ refer to the initial and final density in the deformed state.

The following materials parameters for Al and W used in calculations are presented in Table I; they were taken from [25]. Another important variable to have in mind is the modification to Y_{max} in order to reduce material dissipation; the value used in that case was two orders of magnitude smaller than the real value.

The mesh size in all cases was equal 1×10^{-5} m = 0.01 mm and selected artificial viscosity resulted in a shock width in Al, W being at least ten times smaller than the smallest-layer thickness in the laminate (0.5 mm). This assures that a steady state is reached behind shock waves when they propagate inside each layer on the initial stage of pulse formation following the impact. Of course it is desirable that the shock width is similar to the one found in experiments [26–28], but the width of the shock front is not important for the parameters of the final state as long as the shock width is significantly smaller than the layer thickness. This ensures that the material reaches Hugoniot states at shock loading in each layer. The Hugoniot states are characteristic for stationary shocks and are independent of the specific mechanisms of dissipation defining resulting shock width. The plastic shock width (Δx) and the rise time (Δt) at a shock stress of 70 GPa were equal to $\Delta t = 3.72 \times 10^{-9}$ and $\Delta x = 3.38 \times 10^{-5}$ m for aluminum and $\Delta t = 9.69 \times 10^{-9}$ and $\Delta x = 4.79 \times 10^{-5}$ m for tungsten. Both of the shock widths are about ten times smaller than the smallest-layer thickness in the laminate (0.5 mm), which assures that Hugoniot states behind the shock are reached inside each of the layers on the initial stage of pulse formation.

We validated results of LS-DYNA calculations with selected material properties based on comparison of the final thermodynamic states behind shock waves with available Hugoniot data. The comparison demonstrated that the model used correctly predicts the stress and specific volume in the simulation of single shock in individual materials. Even more important is that the simulations correctly predict the temperatures on the Hugoniots and also the temperatures after unloading for Al and W. This numerical approach was used to investigate the nature of relatively short, high-amplitude stress pulses in the Al-W laminate.

III. RESULTS OF NUMERICAL CALCULATIONS

The nature of the short stress pulses of different durations excited by the impact of an Al plate with thicknesses of 2 and 8 mm propagating in the laminate materials with different cell sizes at various distances from the impact side is presented below. The main focus is on the nature of the pulses generated at various conditions of loading and to discover the nature of propagating pulses and scaling that might be generated by the interplay between duration of impact controlled by the thickness of impactor and cell in the laminate materials. The main characteristic time scaling is determined by the ratio (t_r) of the duration of the incoming pulse and the duration of propagation time through the cell approximated by

$$t_r = \frac{2d_{\text{imp}}}{C_{\text{imp}}} \Big/ \frac{d_{\text{lam}}}{C_{\text{lam}}}, \quad (9)$$

where d_{imp} and d_{lam} are the size of the impactor and size of the cell in the laminate respectively; c_{imp} and c_{lam} refer to the sound speed of the impactor and the laminate. For the sound speed in the laminate, we use the definition for the average sound speed in a laminate found in [16,29]. This definition is later used in the theoretical approach developed in this paper. The final expression for the time ratio is

$$t_r = \frac{2d_{\text{imp}}}{C_{\text{imp}}}\sqrt{\frac{d_{\text{Al}}^2}{C_{\text{Al}}^2} + \frac{d_{\text{W}}^2}{C_{\text{W}}^2} + \left(\frac{Z_{\text{Al}}}{Z_{\text{W}}} + \frac{Z_{\text{W}}}{Z_{\text{Al}}}\right)\left(\frac{d_{\text{Al}} d_{\text{W}}}{C_{\text{Al}} C_{\text{W}}}\right)}, \quad (10)$$

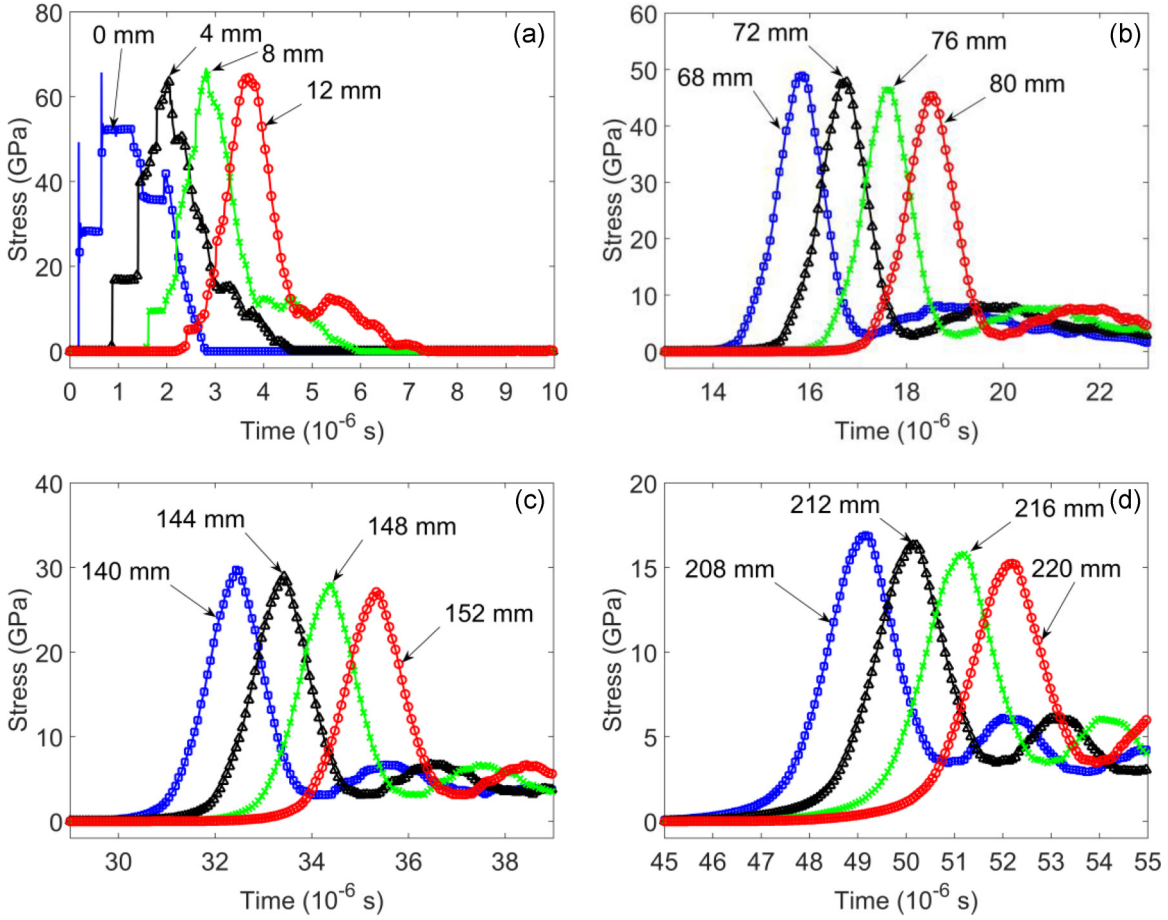

FIG. 2. (Color online) Stress pulse evolution in 2 + 2 laminate; data correspond to the interfaces of Al-W layers at different depths: (a) 0, 4, 8, and 12 mm; (b) 68, 72, 76, and 80 mm; (c) 140, 144, 148, and 152 mm; (d) 208, 212, 216, and 220 mm. The pulse was generated by the impact of an 8-mm Al plate at a velocity of 2800 m/s.

where d_{Al} and d_{W} refer to the Al and W layer sizes of the laminate, Z_{Al} and $Z_{\mathrm{W}}(Z_i = \rho_i C_i)$ represent the acoustic impedance of each layer, and finally C_{Al} and C_{W} are the corresponding sound speeds of each layer. For all our studied cases $C_{\mathrm{imp}} = C_{\mathrm{Al}}$ but d_{imp} has values of either 2 or 8 mm. From here on, the laminated materials are referred to as 2 + 2, 1 + 1, and 0.5 + 0.5 laminates, corresponding to 4−, 2−, and 1-mm cells. All the laminates were loaded by impact of the Al plate at velocity 2800 m/s and FWHM refers to full width at half maximum.

A. 2 + 2 Al-W laminate, impact by 8-mm Al plate

The impact loading of the 2 + 2 laminate by Al impactor with the thickness 8 mm corresponds to the value of t_r equal to 2.5. In these calculations real materials properties presented in the Table I were used. Figures 2(a)–2(d) show that these conditions of impact did not result in a steady state shock wave in the laminate because the duration of the incoming pulse was too short.

Shock waves in each of the layers are clearly distinguishable at depths up to 8 mm from the impacted end. We observe the formation of a qualitatively unique pulse (not a shock wave) mainly formed at the distance 12 mm from the impacted end [Fig. 2(a)]. It has a width close to only three cell sizes with a small amplitude tail. It is clear from Figs. 2(a)–2(d) that formation of the main pulse is caused by multiple reflection of leading stress pulses on Al-W interfaces mostly balanced by nonlinearities of the Al and W behavior. The tail is due to the dissipative properties of the materials.

The dispersion originates from multiple shock wave reflections from interfaces clearly seen in Fig. 2(a).The main pulse propagates with decreasing amplitude being equal to 65 GPa at a depth of 12 mm and about 15 GPa at a depth of 220 mm. This decrease of amplitude is accompanied by an increase of the main pulse space width (FWHM increased about 40%). At larger depths the main pulse is accompanied by an oscillatory tail and at the relatively short distances, e.g., from 68 to 80 mm, the whole pulse can be considered as quasistationary with a similar profile but decreasing amplitude [Fig. 2(b)].

It is very important to remark that the observed main localized pulse with characteristic length comparable to the cell size of the laminate was formed in dissipative media. The rate of dissipation in our calculations matches real losses of energy, unlike in previous papers where no dissipation was taken into account [16–18,20–22]. It is essential to point out that this "real" dissipation does not prevent formation of a prime localized wave in our conditions of loading, and it only results in its attenuation.

We can see that the mesostructure and nonlinear properties of a laminate resulted in dramatic transformation of the initial shock wave into a localized pulse with a different path of loading in comparison with the shock wave. As a result, temperatures corresponding to the maximum stresses are significantly different than at the same stresses in the shock wave. For example, a shock wave at a stress of 55 GPA in Al results in a temperature equal to 1471 K versus a temperature of 650 K in the localized pulse.

We conducted simulations at relatively small amplitude of stress pulses generated by impact of 280 m/s flyer Al plate in Al-W laminate with "normal" dissipation. The propagating stress pulse generated by this impact exhibits a tendency to localize, but attenuates very rapidly developing an attached oscillating tail instead of a quasistationary pulse observed at higher amplitudes of the stresses [Fig. 2(b)].

The formation of the localized pulse with a smooth front is beneficial for shock protection because it prevents spall on the free surface.

B. 2 + 2 Al-W laminate with artificially small Y_{max}, impact by 8-mm Al plate

We now investigate the laminate with the same mesostructure but with reduced maximum yield strength Y_{max} of the materials thus causing plastic flow to occur at lower stress levels reducing dissipation. This case helps us to clarify the role of plastic deformation on the formation of the pulse. It is possible to observe that close to the impacted side the same dispersion and nonlinearity shapes the leading wave as in the previous case [compare Fig. 2(a) with Fig. 3(a)].

Figure 3(a) shows the initial steps in development of the solitarylike pulse through multiple shock reflections. Figure 3(b) demonstrates the persistence of the kinks on the fronts of practically formed solitarylike pulses and their slow separation from their tails, and Fig. 3(c) presents solitarylike pulses separated from their tails with relatively slow disappearance of kinks on the fronts of stress profiles at appropriate distances from the entrance. Finally, Fig. 3(d) shows the stationary solitarylike pulses completely separated from their tails and without kinks on the front parts. In the case of material with real properties we formed a quasistationary attenuating oscillatory wave profile [Figs. 2(a)–2(d)], unlike solitarylike waves at low dissipation (Fig. 3).

It is interesting to compare pulses in material with real dissipative properties, near the impacted end; pulses with similar amplitude in artificially-low-dissipative materials; and pulses of similar amplitude where the laminate behaves elastically (Fig. 4). Figure 5 demonstrates that these pulses at similar maximum amplitudes (taken at different distances

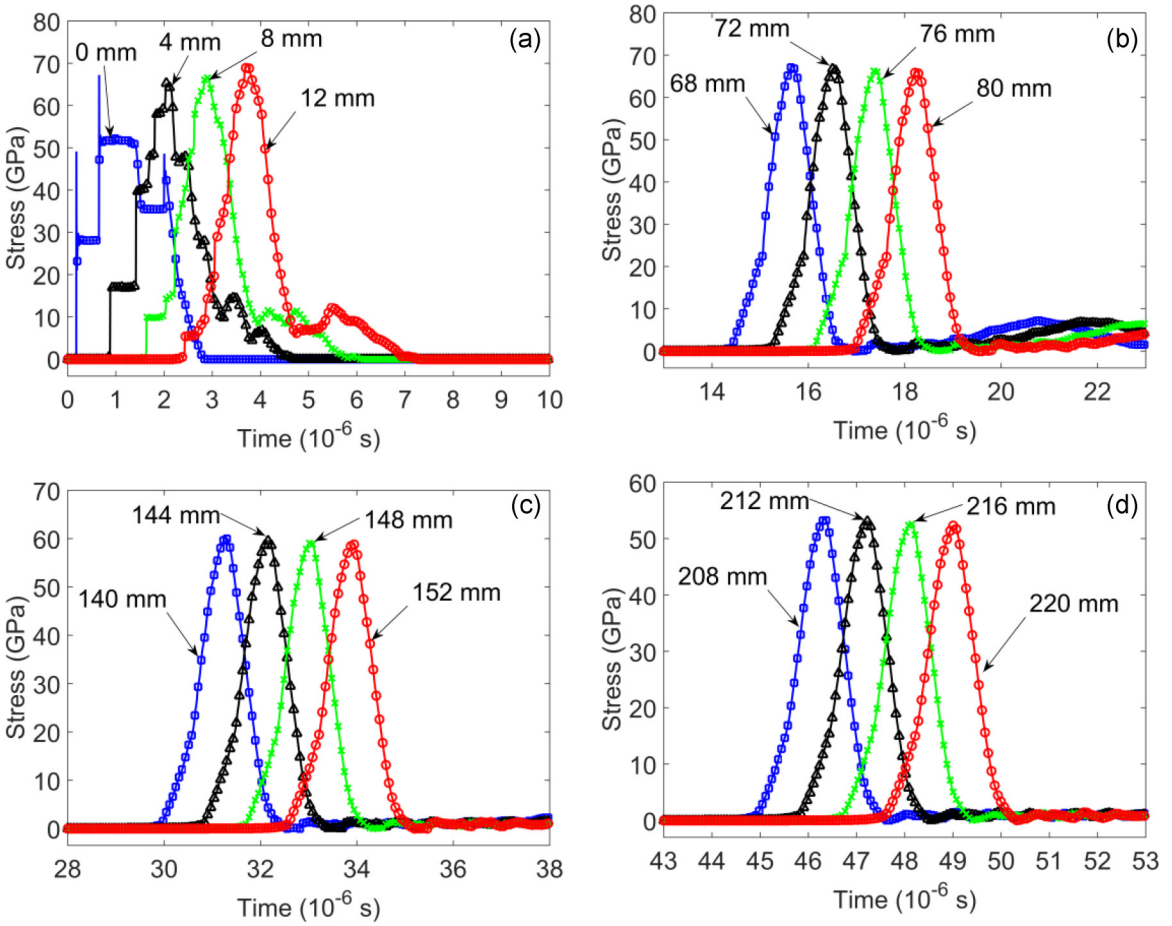

FIG. 3. (Color online) Stress pulse evolution in 2 + 2 laminate with artificially small Y_{max}; data correspond to the interfaces of Al-W layers at different depths: (a) 0, 4, 8, and 12 mm; (b) 68, 72, 76, and 80 mm; (c) 140, 144, 148, and 152 mm; (d) 208, 212, 216, and 220 mm. The pulse was generated by the impact of an 8-mm Al plate at a velocity of 2800 m/s.

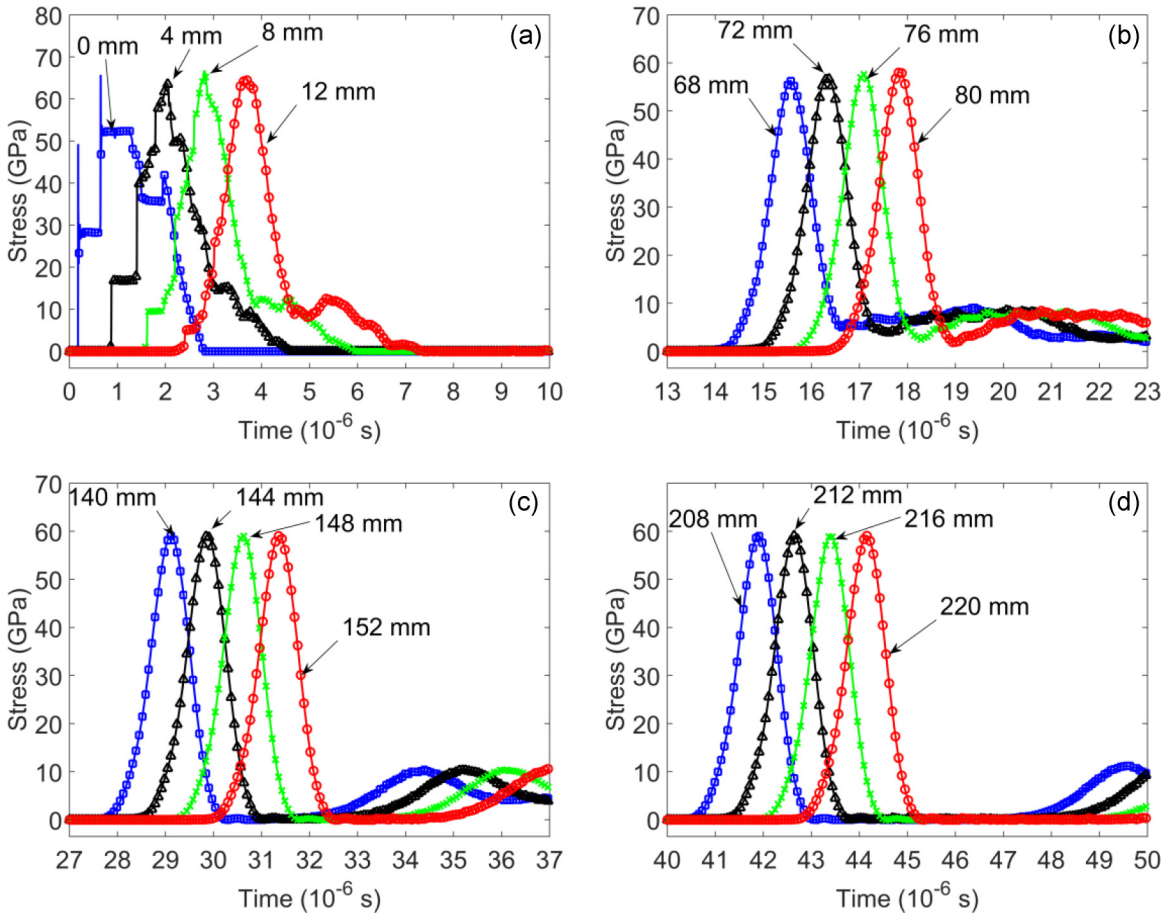

FIG. 4. (Color online) Stress pulse evolution in 2 + 2 laminate; data correspond to the interfaces of Al-W layers at different depths: (a) 0, 4, 8, and 12 mm; (b) 68, 72, 76, and 80 mm; (c) 140, 144, 148, and 152 mm; (d) 208, 212, 216, and 220 mm. The pulse was generated by the impact of an 8-mm Al plate at a velocity of 2800 m/s. Initial length of the laminate with real dissipative properties was 64 mm; it was in contact with a pure elastic laminate with identical mesostructure.

from the impacted side, 40 mm for real properties, 156 mm for artificially low dissipation, and 80 mm for the elastic case) are almost identical. In the case of the material with artificially low maximum yield strength there is a slight difference in the pulse shape—the front of the wave has a clear kink that does not disappear until the pulse has traveled about 200 mm [Fig. 3(d)]. To understand how these pulses propagate in a pure elastic laminate, we ran calculations with real dissipative properties up to the propagation distance where the quasistationary pulse was formed after traveling the distance of 64 mm and after that it transmitted into the pure elastic material with identical mesostructure. The pulse in pure elastic materials propagated initially with relatively small changes (amplitude increase from initial value of 55–59 GPa), quickly approaching the steady state after a distance of about 11 cells (Fig. 4).

Thus it is possible to conclude that the leading pulse in a dissipative material even at relatively large distances from the impacted end (Figs. 2–4) is dominated by the combination of dispersion and nonlinearity, and cell size dictates the spatial dimension of this stress pulse (FWHM of the pulse is equal to 1.17 cell sizes).

Despite the similarity of stress pulses (Fig. 5) we may observe different temperatures due to the difference in dissipative properties. The time dependence of the stresses and temperatures in the localized pulse propagating in the 2 + 2 laminates with different dissipative properties is presented in Fig. 6. It is clear that the amplitude decrease in both cases

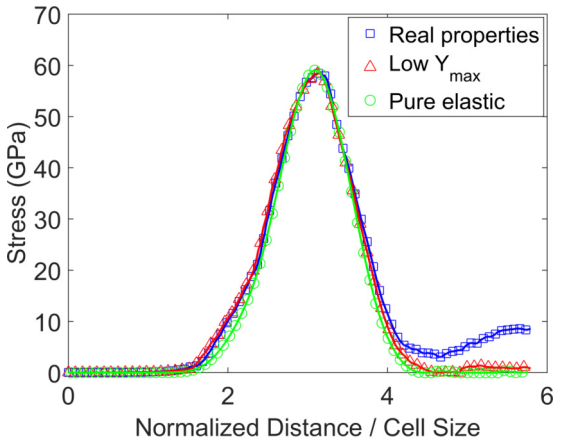

FIG. 5. (Color online) Comparison of wave shape at same stress amplitude of 58 GPa generated by the impact of an Al plate with thickness 8 mm for the case of a 2 + 2 laminate with real dissipative properties, laminate with an artificially small Y_{max}, and laminate with elastic behavior.

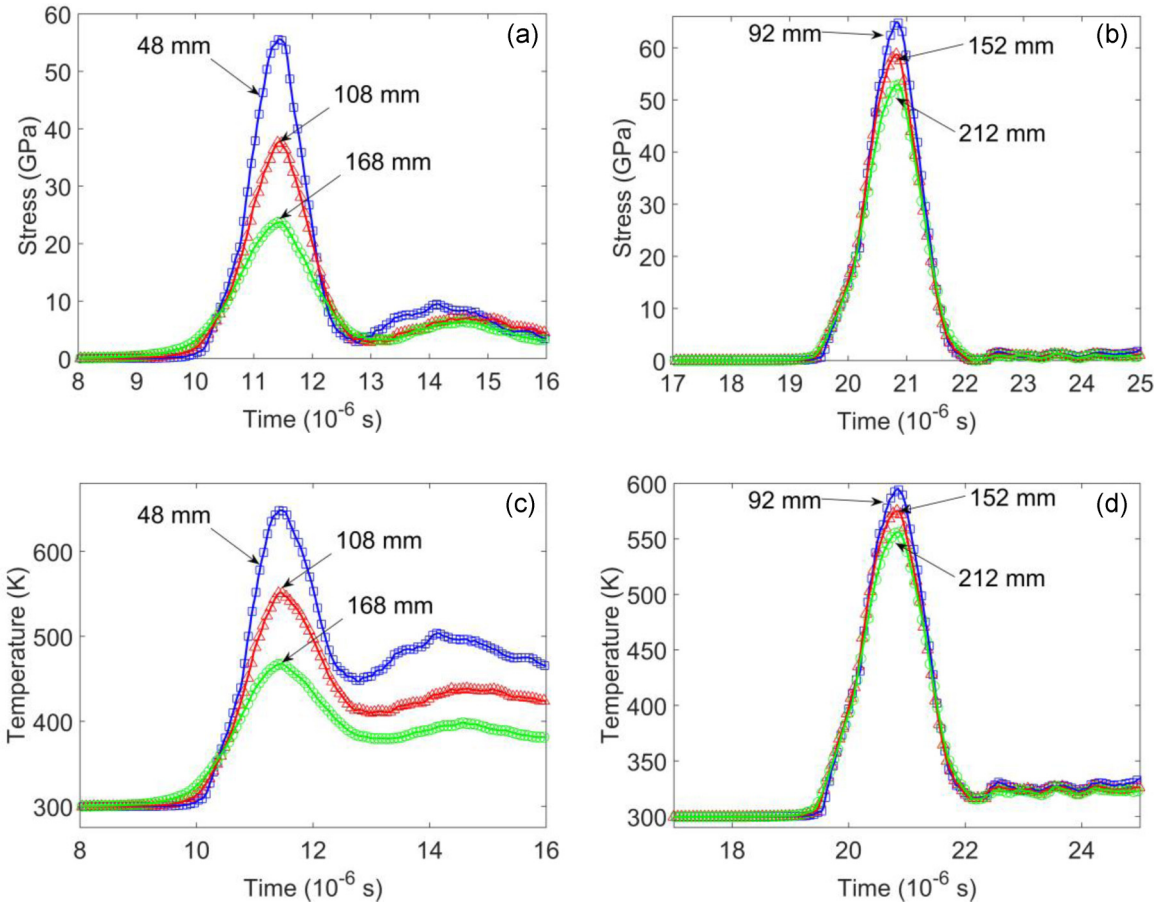

FIG. 6. (Color online) Comparison of attenuating stress traveling waves generated by the impact of an Al plate with 8 mm thickness in a $2+2$ laminate and their corresponding temperatures in Al layer: (a,c) Laminate with real material properties and (b,d) laminate with an artificially small $Y_{\max}$.

(less in the material with an artificially small $Y_{\max}$) did not significantly change the pulse duration time and in the case of the material with smaller dissipative properties the shape of the pulse was maintained practically the same, with the FWHM change being only about 3%. This agrees with the previous conclusion that the pulse shape is determined mostly by nonlinearity and dispersion with dissipation affecting mostly amplitude.

Though nonlinearity and periodic mesostructure in real materials are able to support the localized pulse with the shape similar to the less dissipative case, the important feature in the former laminate is the significant residual temperature, about half of the maximum temperature [Fig. 6(c)]. This behavior emphasizes the difference of this localized wave with classical solitary wave in which material returns to its initial state after being dynamically compressed.

It is very important to emphasize that the maximum temperatures at these waves are significantly smaller than temperatures in the shock waves at the same amplitude. In the material with real dissipative properties at maximum stress of 55 GPa in a quasistationary localized wave, increase of the Al temperature was 350 K [Fig. 6(c)], which is more than three times smaller than the increase of temperature in the shock wave in Al at the same pressure (1171 K); the initial temperature was 300 K.

The difference in temperature increase after unloading is also dramatic—after unloading of the quasistationary localized pulse with amplitude of 55 GPa, the increase of residual temperature over initial temperature was about 150 K, versus an increase of residual temperature being 493 K after shock loading with the same stress amplitude and subsequent unloading.

If we consider a whole pulse with leading amplitude of 55 GPa (including the tail) as a quasistationary shock wave then the estimate of the temperature increase at the tail with stress of 4 GPa [Fig. 6(a)] will be equal 30 K (corresponding to shock stress of 4 GPa), which is much smaller than 170 K in the tail of the localized wave [Fig. 6(c)]. Thus a complex quasistationary pulse with two maxima cannot be considered as a stationary shock wave.

These comparisons demonstrate that under considered impact loading the temperature estimations based on the Hugoniot of components using dynamic pressures are not adequate. Because the localized pulses provide shockless compression of Al and W it is interesting to compare the maximum calculated temperatures with the temperature corresponding to isentropic compression. For Al at 55 GPa the estimate of the isentropic temperature increase is equal to 227 K [30], which is smaller than the calculated temperature increase of 350 K in a localized wave [Fig. 6(c)]. The estimated

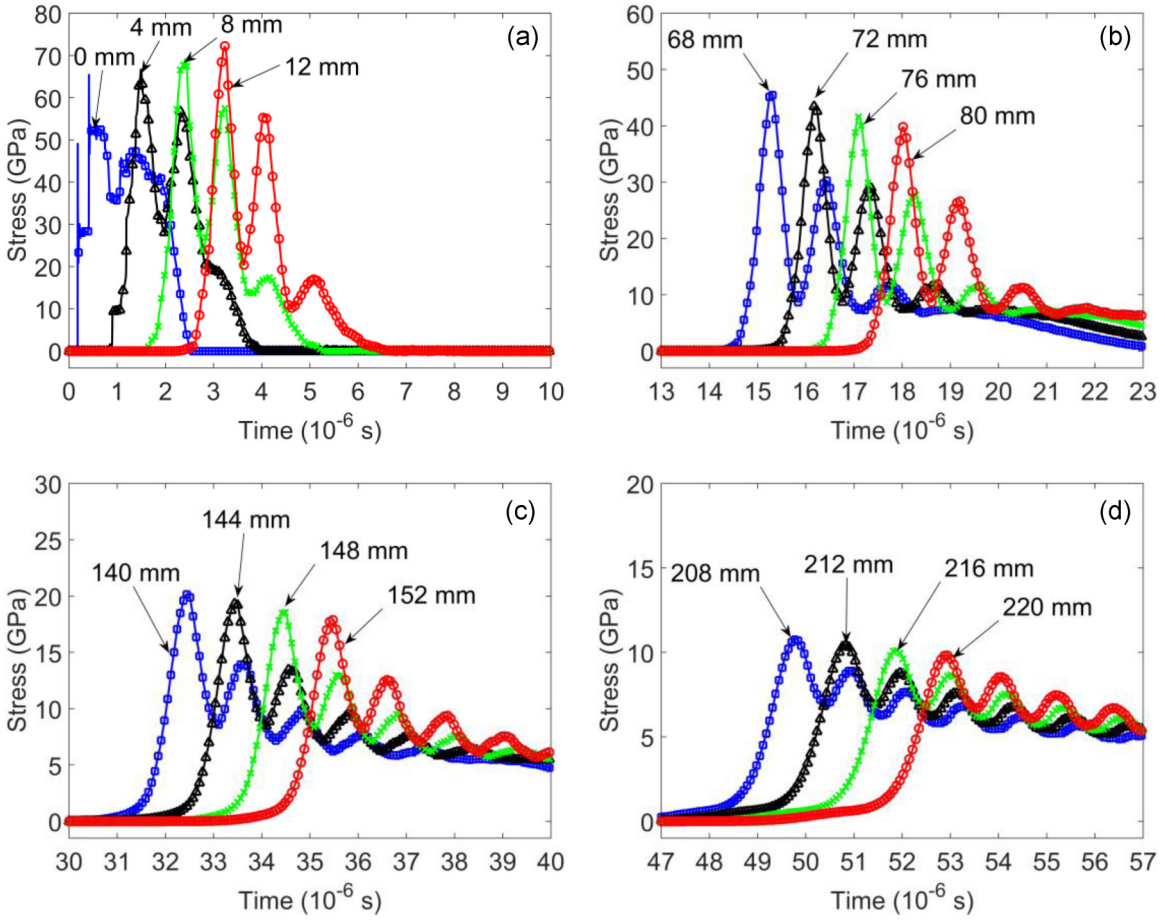

FIG. 7. (Color online) Stress pulse evolution in $1 + 1$ laminate; data correspond to the interfaces of Al-W layers at different depths: (a) 0, 4, 8, and 12 mm; (b) 68, 72, 76, and 80 mm; (c) 140, 144, 148, and 152 mm; (d) 208, 212, 216, and 220 mm. The pulse was generated by the impact of an 8-mm Al plate at a velocity of 2800 m/s.

temperature in isentropic compression is much closer to the calculated temperature in localized wave than temperature at shock loading at the same pressures. Thus temperatures under isentropic compression give the reasonable lower estimate of the maximum temperatures in localized waves.

C. 1 + 1 Al-W laminate, impact by 8-mm Al plate

It is interesting to determine if the shape and amplitude of the localized pulse observed in previous calculations is scaled with the size of the cell in laminates or is simply determined by the incoming pulse. To clarify this point we calculated the wave evolution inside a $1 + 1$ mm laminate with real dissipative properties generated by the same impact as in the case of a $2 + 2$ laminate. The thickness of the impactor was the same, but the time ratio of the impactor to the cell was larger than in the previous case. This also allows us to investigate if the number of localized pulses depends on the time ratio. For example, in the case of strongly nonlinear waves in granular materials [9] a single solitary wave was excited when the mass of the impactor was equal to the mass of the particle and multiple solitary waves were generated at the larger mass of the impactor. However, the nature of the propagating pulse can be strongly influenced by the dissipative properties of the dispersive media [9,31,32].

The impact of an 8-mm Al plate on this $1 + 1$ laminate corresponds to the time ratio of the impactor to cell size being equal to 5.1, which is about two times larger than in the previous case of the $2 + 2$ laminate. Also it is interesting to see if the decrease of the cell size at the same impactor mass results in faster formation of localized pulses and if the corresponding distance for the formation of such pulses is scaled with the cell size.

The evolution of the wave at different depths is presented in Fig. 7. The impact with this impactor to cell time ratio of 5.1 demonstrated a tendency to the formation of multiple pulses close to the impacted end. Nevertheless, the dissipative properties of the material prevent the formation of the train of solitarylike waves. Instead an oscillatory triangular profile was observed at larger depths [Figs. 7(c) and 7(d)].

There is a difference between maximum amplitudes of stress in these pulses at similar depths of 220 mm. For example, the amplitude of the leading pulse is equal to 15.2 GPa for the $2 + 2$ laminate versus 9.8 GPa for the $1 + 1$ laminate, despite the same impact and the same average density of laminates. This difference is apparently due to the difference in their dispersive properties resulting in generation of multiple solitarylike waves in the laminate with smaller cell sizes. This demonstrates that amplitudes of the stress pulses can be

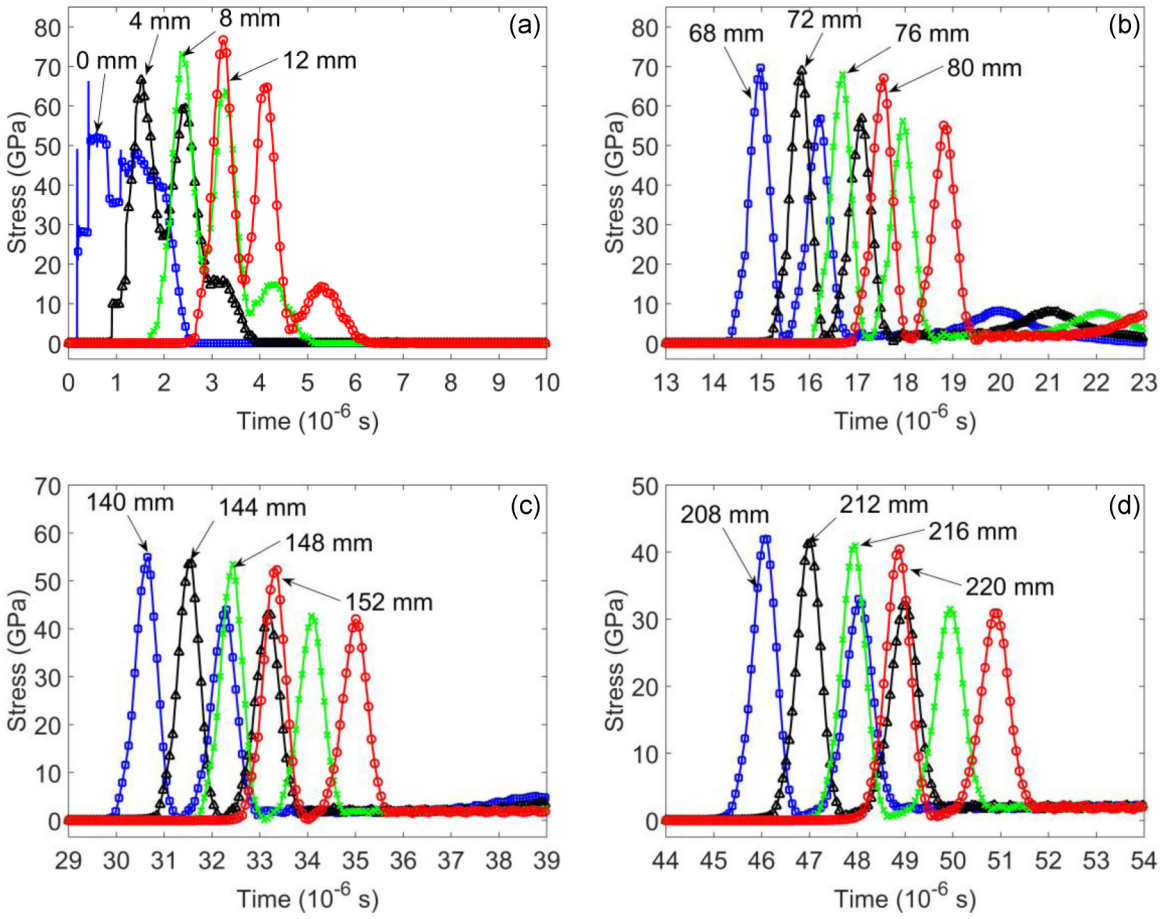

FIG. 8. (Color online) Stress pulse evolution in $1+1$ laminate with artificially small $Y_{\max}$; data correspond to the interfaces of Al-W layers at different depths: (a) 0, 4, 8, and 12 mm; (b) 68, 72, 76, and 80 mm; (c) 140, 144, 148, and 152 mm; (d) 208, 212, 216, and 220 mm. The pulse was generated by the impact of an 8-mm Al plate at a velocity of 2800 m/s.

decreased by decreasing cell size in laminates, which results in multiple solitarylike waves with small amplitude instead of a single one with a larger amplitude.

At the depths where the quasistationary pulse is observed (68–80 mm), the ratio of its characteristic scales to cell size (FWHM$/d = 1.25$ and $(0.1-0.9)\Delta/d = 1.15$) are similar to those observed for the $2+2$ laminate, demonstrating their scaling with the laminate cell size.

D. $1+1$ Al-W laminate with artificially small $Y_{\max}$, impact by 8-mm Al plate

We saw in the previous section that dissipative properties may be responsible for the triangular oscillating wave profile preventing formation of a train of separate solitary waves. To clarify the role of dissipation we investigated the nature of the wave generated at the same impactor to cell time ratio (5.1), but introducing artificially small yield strength and the reduction of the dissipation. It is clear that reduced dissipative characteristics of the components facilitated the separation of the train of localized pulses (Fig. 8). They travel with different speeds depending on their amplitude and resemble a train of weakly attenuating solitarylike waves. This behavior is contrary to the previous case where a quasistationary strongly attenuating triangular oscillatory profile was formed at identical conditions of impact (Fig. 7).

We consider the formation of a quasistationary solitarylike wave when the stress in the wave reached 10% of its maximum on the release part. Following this agreement we observed that its formation occurs fairly fast (at about 26 mm in depth) after traveling 13 cells. The apparently longer distance for establishing a stationary solitarylike pulse in this case, in comparison with impact on a $2+2$ laminate, with the same thickness of impactor is due to the presence of the second wave following the first one.

The FWHM width of the localized pulse was equal to 1–1.25 times the cell size depending on amplitude, which is similar to the width of the localized pulse in $2+2$ laminate in nondissipative and dissipative cases (Fig. 8).

E. $0.5+0.5$ Al-W laminate, impact by 8-mm Al plate

It is interesting to investigate the characteristic scale of localized pulses in relation to cell size and their number and distance at which they are formed in the laminate with reduced cell size under the same impact (duration of incoming pulse). The impactor to cell time ratio was increased to 10.2 by reducing the cell size to 1 mm ($0.5+0.5$ mm layered material) and keeping the duration of the incoming pulse the

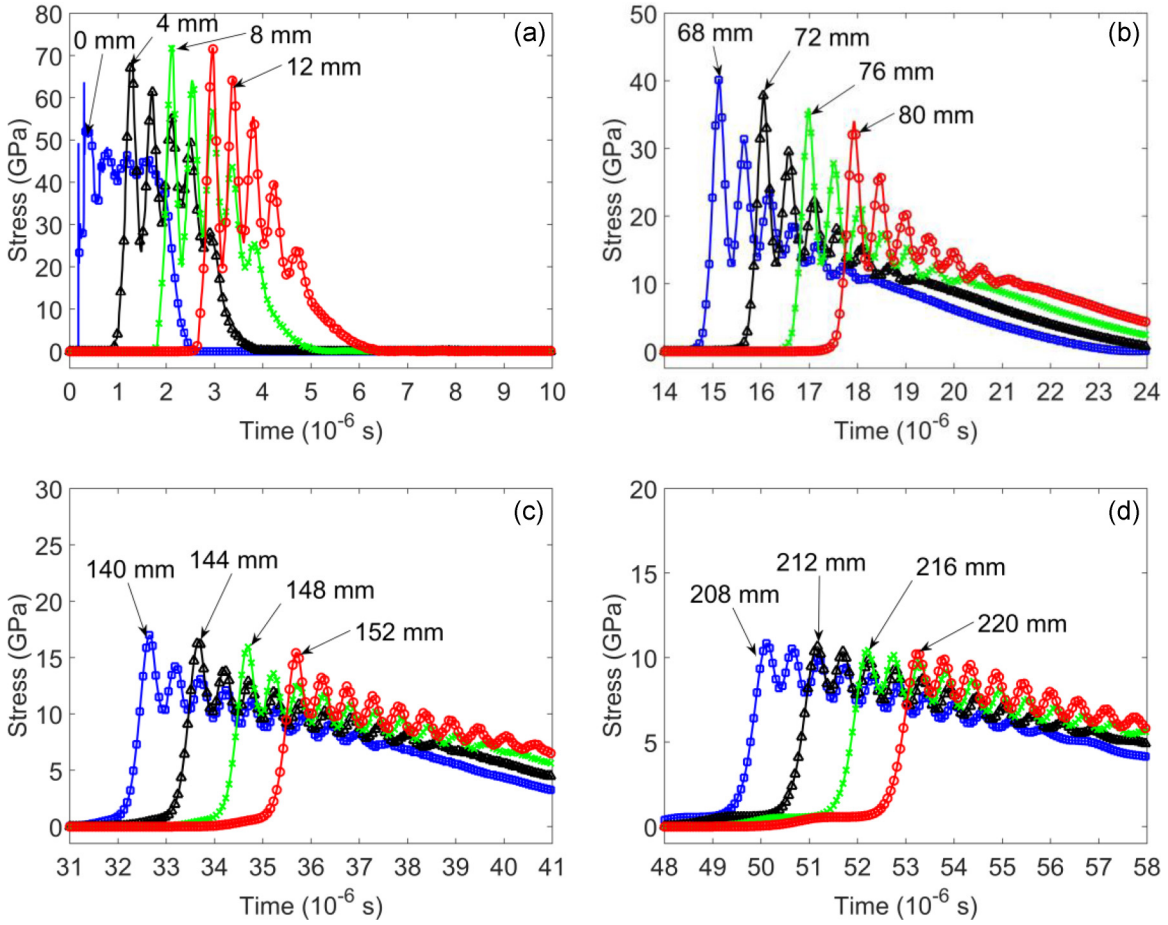

FIG. 9. (Color online) Stress pulse evolution in $0.5 + 0.5$ laminate; data correspond to the interfaces of Al-W layers at different depths: (a) 0, 4, 8, and 12 mm; (b) 68, 72, 76, and 80 mm; (c) 140, 144, 148, and 152 mm; (d) 208, 212, 216, and 220 mm. The pulse was generated by the impact of an 8-mm Al plate at a velocity of 2800 m/s.

same (thickness of Al impactor, 8 mm). The results should be compared with the cases where $2 + 2$ and $1 + 1$ laminates were impacted by the 8-mm-thick Al plate at the same velocity (Figs. 2 and 7).

In the case of the $0.5 + 0.5$ laminate, an oscillating triangular pulse was formed indicating the tendency to create the train of five localized waves Fig. 9(a), instead of one pulse (in the $2 + 2$ laminate, $t_r = 2.5$) and three pulses (in the $1 + 1$ laminate, $t_r = 5.1$) in the previous cases, also with real dissipative properties of the components (Figs. 2 and 7). It should be mentioned that at a time ratio equal to 2.5 a single quasistationary pulse was formed (Fig. 2) and at a time ratio of 5.1 an oscillatory attenuating triangular pulse was observed (Fig. 7). These results prove that there is a strong correlation between shapes of wave profiles generated by the same impact at different time ratios. The time ratio determines the ratio of the characteristic time of the incoming load and the time scale determined by mesostructure, e.g., the time of wave propagation through the cell or the time duration of corresponding quasistationary pulses.

In weakly nonlinear and strongly nonlinear discrete materials there is a value of critical viscosity corresponding to the transition from oscillatory stationary shock profile to monotonous shock [33]. It seems that in the case of laminates there is a value of yield strength $Y_{\max}$ that will prevent splitting of the initial pulse into a train of solitary waves resulting in oscillatory or monotonous shocklike pulse.

Because different wave profiles were formed in laminates with different cell sizes at the same impact, it is interesting to compare the effectiveness of each laminate to decrease the amplitude of the leading pulse (it should be mentioned that decrease of cell size may result in the opposing effect and cause an increase of the amplitude of the leading pulse [14] [see also Figs. 2(a), 7(a), and 9(a)]. The amplitudes of the leading pulses in laminates with different cell sizes, at the same depth of 220 mm, were equal to 15.2 GPa ($2 + 2$ laminate), 9.8 GPa ($1 + 1$ laminate), and 10.3 GPa ($0.5 + 0.5$ laminate). Although there is a small difference between the amplitudes for the $1 + 1$ mm and $0.5 + 0.5$ (with slight increase of amplitude in the latter case), the amplitude in the $2 + 2$ layered composite is about 50% larger. This difference in the amplitudes of the leading wave can be explained due to the changes on dispersive properties of the laminate without changing the dissipative and nonlinear properties of the components. These data also demonstrate that amplitude of the leading pulse cannot be reduced indefinitely with reduction of the cell size.

Some very interesting phenomena of the increase of the duration of the triangular pulse in the $0.5 + 0.5$ laminate should be mentioned (compare Figs. 7 and 9). We will see

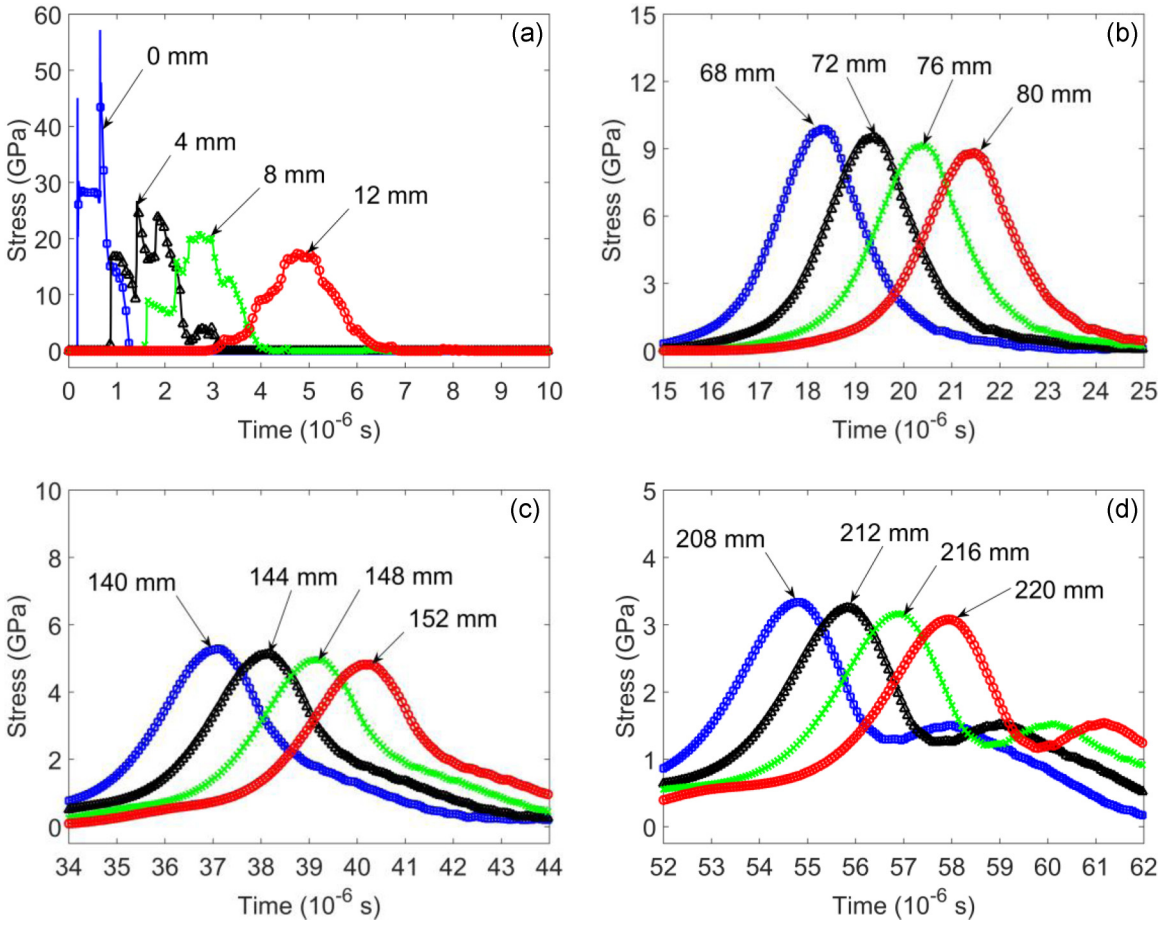

FIG. 10. (Color online) Stress pulse evolution in 2 + 2 laminate; data correspond to the interfaces of Al-W layers at different depths: (a) 0, 4, 8, and 16 mm; (b) 68, 72, 76, and 80 mm; (c) 140, 144, 148, and 152 mm; (d) 208, 212, 216, and 220 mm. The pulse was generated by the impact of a 2-mm Al plate at a velocity of 2800 m/s.

later that this is directly connected to the dispersive properties of the laminates.

The characteristic (0.1–0.9) space scale of the main leading front of the oscillating triangular wave at large depths is scaled with the cell size being equal to about 1.1 cell sizes [Fig. 9(b)]. This scaling is similar to the size of the leading front in the 1 + 1 laminate [Fig. 7(b), 1.1 cell size]. It is interesting that in this laminate we observe the dispersive elastic precursor whose length is increasing with propagation distance [Fig. 12(d)].

F. Al-W 2 + 2 laminate, Al impactor with thickness of 2 mm

In the case of a 2 + 2 laminate with real material properties, under the impact of an 8-mm Al flyer plate, we observed that a slightly attenuating solitarylike pulse was generated from a relatively long incoming pulse (Fig. 2). It is interesting to see if a similar solitarylike wave could be generated in the same 2 + 2 laminate from different initial conditions (reduced duration of impact by using a 2-mm instead of 8-mm Al flyer plate; in this case the time ratio between the impactor and the cell is 0.6). We could expect that shorter duration impact may create a similar solitarylike pulse if the laminate under high-amplitude loading behaves as a classical weakly dissipative nonlinear dispersive medium.

Figures 10(a)–10(d) show the evolution of the stress profile as a result of the impact of the Al plate with a thickness of 2 mm on the 2 + 2 laminate. It is clear that the localized pulse is also formed at the distance of about 24 mm from impacted end (not shown in the figures). This process required a considerably longer distance than 12 mm in the 2 + 2 laminate impacted by an 8-mm Al plate (compare Fig. 10 with Fig. 2).

Contrary to what we observed in the case with an 8-mm impactor, the amplitude of the formed solitarylike pulse was smaller (compare Figs. 2 and 10). This could be due to the smaller linear momentum and energy in the case of a 2-mm Al striker, but as soon as a solitarylike pulse was formed (with FWHM equal to about two cells and 0.1–0.9 ramp size being close to two cells also) it was practically identical to the leading part of the same amplitude (10 GPa) pulse in the same laminate formed under impact by 8 mm (Fig. 11). It is important to remark that once the amplitude has been greatly reduced (below 5 GPa at the depths larger than 140 mm) an elastic precursor can be observed and the shape of the pulse does not resemble a classic shape of a soliton [Figs. 10(c) and 10(d)].

In this case, the solitarylike waves with low amplitudes at depths 68–80 mm have a FWHM = 2 cell sizes and a 0.1–0.9 ramp size (Δ) equal to 1.9 cell size.

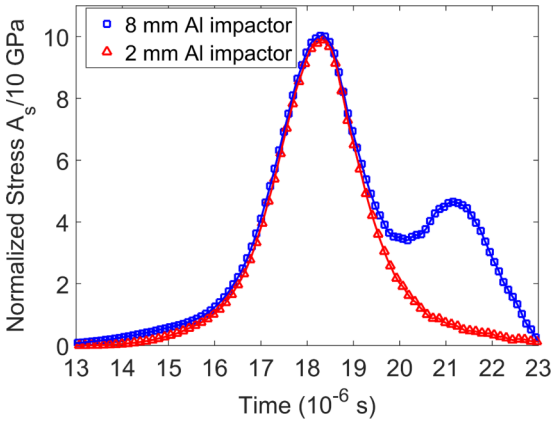

FIG. 11. (Color online) Comparison of shapes of solitarylike wave and leading part of the pulse both formed in $2+2$ laminates with real dissipative properties excited by impact of an Al plate with different thickness, 2 and 8 mm, correspondingly.

It is important to compare localized pulses with similar amplitude propagating in a laminate with the same mesostructure, but excited with different initial conditions (impact by 2-mm Al plate versus 8-mm Al plate).

Figure 11 presents this comparison. It is evident that the resulting attenuating localized pulse has a direct relation to the laminate mesostructure. It is interesting that the rising parts of the localized pulses in the $2+2$ laminate are almost identical though they were excited by impacts of 8- and 2-mm Al plates.

G. 1 + 1 Al-W laminate, impact by 2-mm Al plate

It is interesting to study if the localized pulses will be observed in laminates with different cell sizes under identical impact conditions (2-mm Al plate with velocity 2800 m/s) and if their space scale is scaled with the cell size also. The previous case with impactor to cell time ratio of 0.6 ($2+2$ laminate) resulted in a single solitarylike wave (Fig. 10).

Based on what has been observed in the $2+2$ laminates impacted by 2- and 8-mm Al impactors, we can expect the formation of one or more solitarylike waves. In the case with a $1+1$ laminate, impacted by a 2-mm Al impactor, the time ratio is 1.3. Figure 12 demonstrates that this laminate indeed supports the single solitarylike wave. The localized pulse is completely formed at a depth of about 8 mm [Fig. 12(a)] compared to 24 mm in the case of a $2+2$ laminate impacted by the same 2-mm Al plate [compare Figs. 12(a) and 10(a) at the similar depths]. It is interesting that decrease of cell size

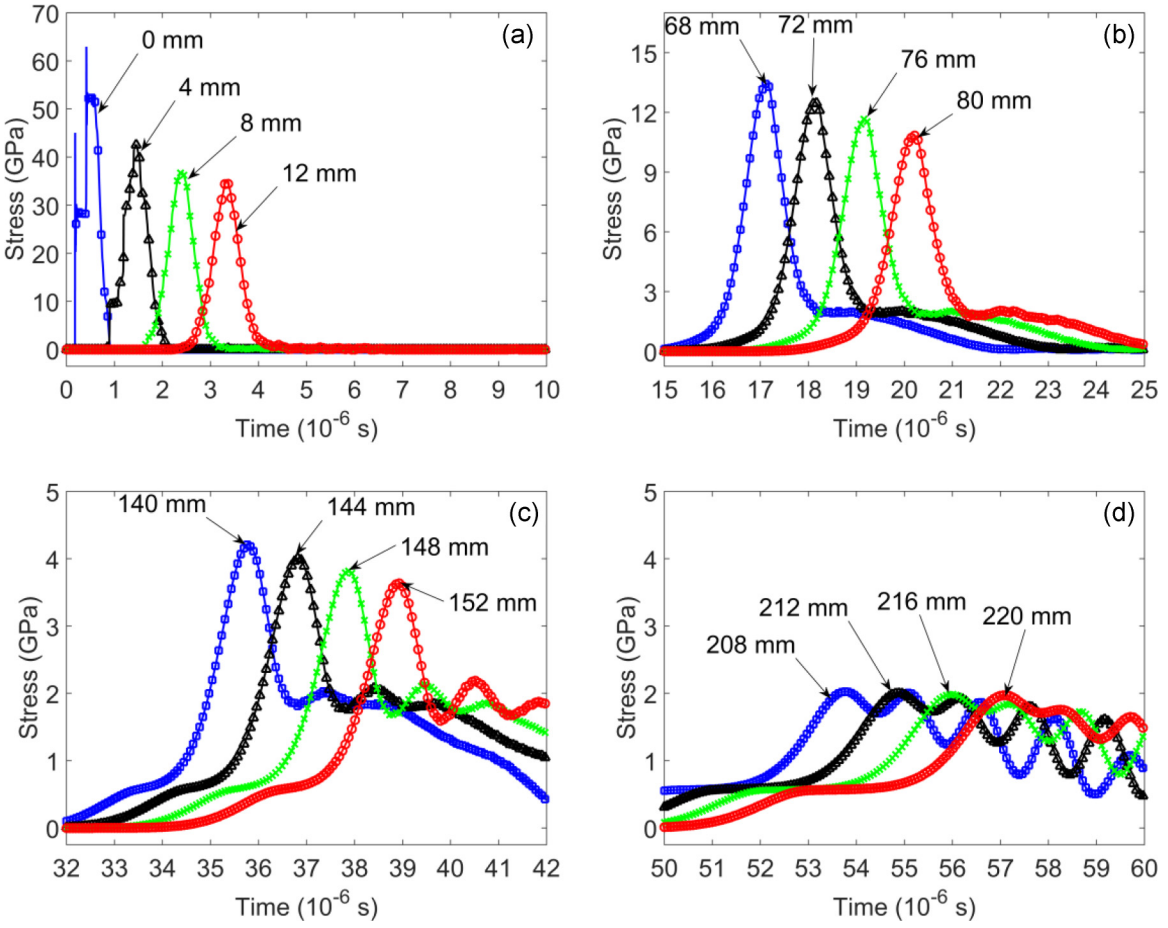

FIG. 12. (Color online) Stress pulse evolution in $1+1$ laminate; data correspond to the interfaces of Al-W layers at different depths: (a) 0, 4, 8, and 12 mm; (b) 68, 72, 76, and 80 mm; (c) 140, 144, 148, and 152 mm; (d) 208, 212, 216, and 220 mm. The pulse was generated by the impact of a 2-mm Al plate at a velocity of 2800 m/s.

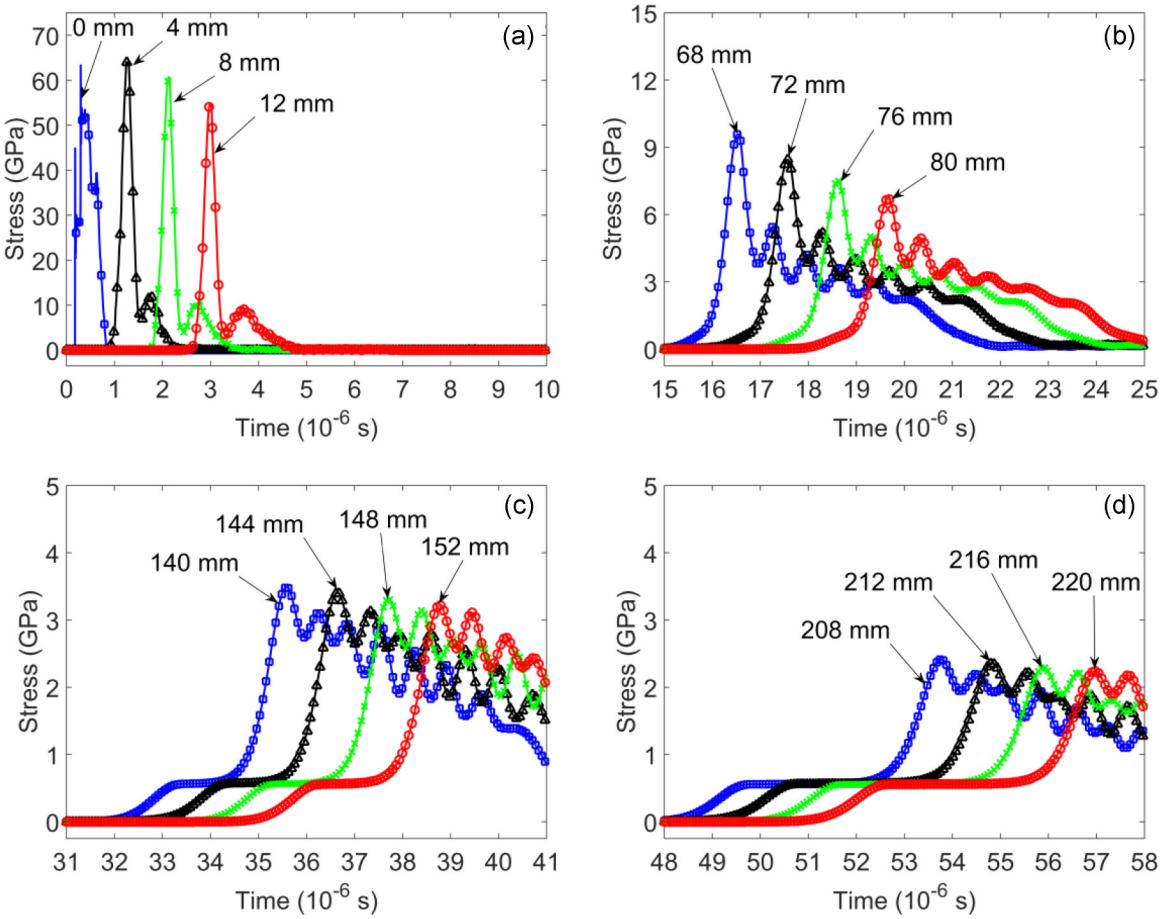

FIG. 13. (Color online) Stress pulse evolution in 0.5 + 0.5 laminate; data correspond to the interfaces of Al-W layers at different depths: (a) 0, 4, 8, and 12 mm; (b) 68, 72, 76, and 80 mm; (c) 140, 144, 148, and 152 mm; (d) 208, 212, 216, and 220 mm. The pulse was generated by the impact of a 2-mm Al plate at a velocity of 2800 m/s.

by two times resulted in the three-times decrease in the travel distance required to form a solitarylike pulse.

It is clear that the shape of the pulse closely resembles a classic solitary wave (bell shape) at a relatively high amplitude of the maximum stress. At lower stress levels [below 5 GPa, Figs. 12(c) and 12(d)], an elastic precursor can be clearly identified and the shape of the wave does not resemble a classic solitary wave and the pulse propagates as an attenuating oscillatory wave. This is consistent with what was observed in the 2 + 2 laminate at low stress levels [Figs. 10(c) and 10(d)]. This occurrence can be explained by the unbalance that exists between the nonlinearities and dispersion at low stress levels. Similar to what was observed before, at low amplitudes at depths of 68–80 mm, the FWHM = 1.8−2 cell sizes and $\Delta = 1.7-1.9$ cell size, which is consistent with the scaling phenomena observed in past cases impacted by a 2- or 8-mm Al plate.

The incoming pulse was quickly transformed into a solitarylike wave at depths of 8 and 12 mm, and at larger depths we observe a leading solitarylike wave followed by a compression tail, if the amplitude of the former was above 10 GPa. This resembles the behavior of a discrete, strongly nonlinear granular chain [31,32] except that strong nonlinearity resulted in decoupling of the leading solitary wave from the compression wave, the latter being converted into a shock wave. The difference between the speed of a solitarylike wave and a compression wave with smaller amplitude in the Al-W laminate is not as large as in a strongly nonlinear granular chain preventing fast coupling of these waves before emerging of the elastic precursor. We can expect a similar behavior if one of the components in the laminate exhibits a strongly nonlinear behavior.

H. 0.5 + 0.5 Al-W laminate, impact by 2-mm Al plate

Laminates (2 + 2 and 1 + 1) impacted by a 2-mm Al plate have shown the capability to form and propagate localized solitarylike pulses (Figs. 10 and 12). It is interesting to investigate if a 0.5 + 0.5 laminate will also support a single solitarylike pulse or their train and what is the travel distance necessary for their formation when impacted by a 2-mm Al flyer plate. In the case where the solitary wave is supported by this laminate, it is interesting to see its shape and characteristic space scale in relation to the cell size and rate of amplitude decay.

The ratio of the characteristic duration of the incoming pulse to the laminate time scale introduced by the mesostructure for this case is 2.5 which is identical to the case of a 2 + 2 laminate impacted by an 8-mm Al plate (Fig. 2). Therefore it is natural to expect the formation of a single solitarylike wave with a small tail behind if the mentioned time ratio is the main

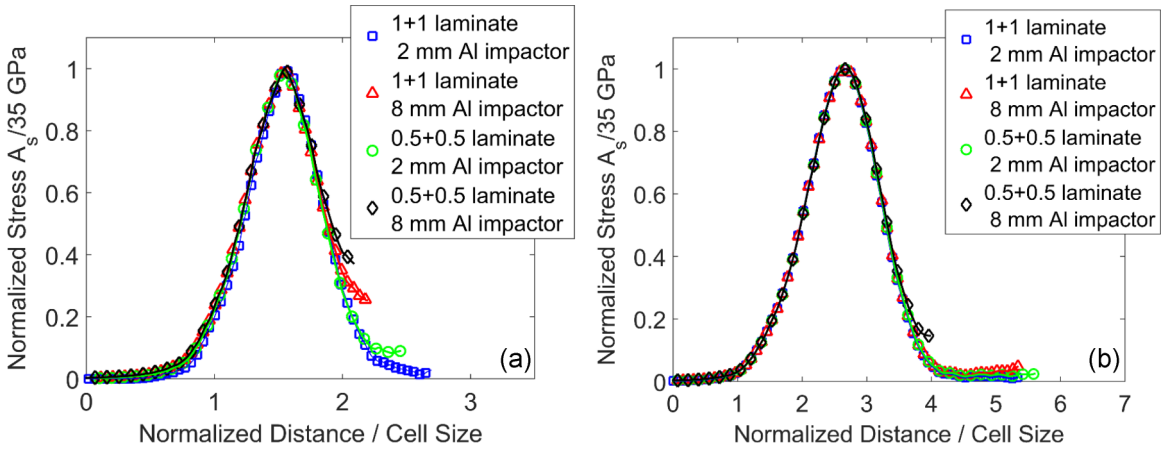

FIG. 14. (Color online) Comparison between the profiles of stress in solitarylike waves with similar amplitudes in Al-W laminates with different cell sizes and dissipative properties generated by two different impactors with thickness of 2 and 8 mm, respectively. The stress is normalized by the following wave amplitudes: (a) Laminates with real dissipative properties: $1+1$ laminate, impacted by 2-mm Al plate, stress amplitude 34.9 GPa; $1+1$ laminate, impacted by an 8-mm Al plate, stress amplitude 34.8 GPa; $0.5+0.5$ laminate, impacted by a 2-mm Al plate, stress amplitude 35.2 GPa; and $0.5+0.5$ laminate, impacted by an 8-mm Al plate, stress amplitude 35 GPa. (b) Laminates with artificially low $Y_{\max}$. $1+1$ laminate, impacted by a 2-mm Al plate, stress amplitude 35.2 GPa; $1+1$ laminate, impacted by an 8-mm Al plate, stress amplitude 35.9 GPa; $0.5+0.5$ laminate, impacted by a 2-mm Al plate, stress amplitude 35 GPa; and $0.5+0.5$ laminate, impacted by an 8-mm Al plate, stress amplitude 35 GPa.

parameter determining the outcome of impact. Evolution of the generated pulse is shown in Figs. 13(a) and 13(d)].

We can see that the incoming pulse was transformed into a fast attenuating leading solitarylike wave followed by a compression wave at a distance of about 4 mm away from the impacted end [Fig. 13(a)]. It is interesting that the traveled distance required to form a solitarylike pulse at the same characteristic duration of the incoming pulse (thickness of impactor) is scaled with the cell size; compare the shapes of pulses in the $0.5+0.5$ laminate at a traveled distance of 4 mm [Fig. 13(a)] in the $1+1$ laminate at a distance of 8 mm [Fig. 12(a)], and in the $2+2$ laminate at a distance of 16 mm [Fig. 10(a)].

This behavior resembles the formation of a two wave structure in a discrete, strongly nonlinear granular chain [31,32] except that a strongly nonlinear interaction between grains resulted in the decoupling of a leading solitary wave from the compression wave, the latter being converted into a shock wave. The absence of separation of these waves in our case is probably due to a relatively small difference between the speed of a leading solitarylike wave and following it, a compression wave with smaller amplitude in the Al-W laminate in comparison with corresponding speeds in a strongly nonlinear chain. We can expect a similar behavior if one of the components in the laminate exhibits a strongly nonlinear behavior.

The strong attenuation of the leading pulse and probably dispersion prevents the formation of a train of localized stress pulses and creates an attenuating oscillatory shock–like profile [Figs. 13(b) and 13(d)] already evident at distances of about 68 mm. At very low stress levels (around 4 GPa) an elastic precursor dramatically changing the shape of the propagating pulse can be observed [Fig. 13(c) and 13(d)], similar to a previous case [Figs. 12(c) and 12(d)], although in the case of the $1+1$ laminate, the elastic precursor appears closer to the impacted end. In this laminate, the scaling of the characteristic sizes of the localized pulse can be observed. At 68–72 mm depth, FWHM $= 1.8-2.2$ cell size and $\Delta = 2.1-2.2$ cell sizes.

I. Comparison of solitarylike wave shapes created by different initial conditions

It is interesting to compare solitarylike waves with similar amplitudes in the same laminate resulting from different initial conditions caused by impactors with different thicknesses. If these waves generated by different initial conditions are quasistationary and similar then it may indicate that they are the result of balancing nonlinear and dispersive properties of the material, as in the case with true solitary waves.

In Figs. 14(a) and 14(b)] normalized profiles of solitarylike waves with similar amplitudes propagating in the Al-W laminates ($1+1$ and $0.5+0.5$) with different dissipative properties, excited by Al impactors with thickness of 8 and 2 mm, are presented. The profiles and durations of the corresponding incoming stress are quite different; for example, the total durations of incoming pulses presented in Figs. 7(a) and 12(a) are 2.35 and 0.74 microseconds, correspondingly.

Four solitarylike waves in normalized coordinates (distance divided by cell size) with very close stress amplitudes are shown in Fig. 14. Figure 14(a) represents the wave profiles propagating in $1+1$ and $0.5+0.5$ laminates with real dissipative properties and similar maximum stresses close to

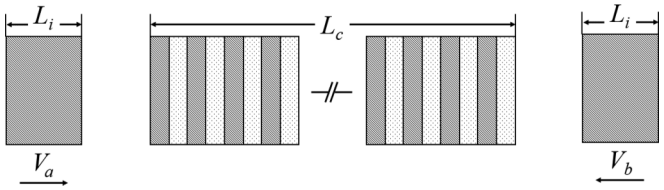

FIG. 15. Laminate impacted at both ends to investigate collision of solitarylike waves.

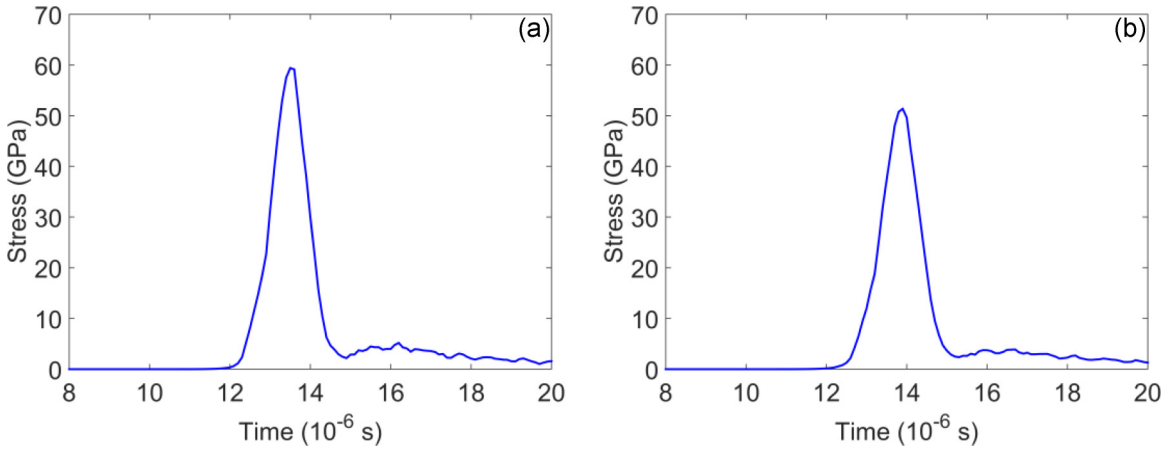

FIG. 16. (Color online) (a) Traveling wave at 60 mm depth from the left end of the laminate with real properties. (b) Traveling wave at 60 mm depth from the right end of the laminate. Both waves are shown before collision.

35 GPa, which were generated by the impact of Al flyer plates with thicknesses of 2 and 8 mm. The respective traveling distances to reach similar amplitudes in these pulses are 40 and 104 mm (1 + 1 laminate) and 32 and 120 mm (0.5 + 0.5 laminate).

Wave profiles with a stress amplitude of about 35 GPa are presented in Fig. 14(b) corresponding to the laminates with reduced dissipative properties (smaller $Y_{\max}$), but with the same mesostructure as in Fig. 14(a). These profiles were formed at depths of 182 mm (1 + 1 laminate), 90 mm (1 + 1 laminate), 60 mm (0.5 + 0.5 laminate), and 92 mm (0.5 + 0.5 laminate), correspondingly, where these quasistationary pulses had similar stress amplitudes.

The comparison among the profiles of these waves demonstrates that they are similar in normalized coordinates despite differences in their dissipative properties. For the case of the laminate with real properties, the FWHM = 1.3 and for the material with small $Y_{\max}$, FWHM = 1.3. This comparison confirms that these waves indeed are a result of the material properties (balancing dispersion caused by the periodic mesostructure and nonlinearity) and do not depend on the initial conditions that generated them, similar to properties of true solitary waves.

J. Head-on collision of solitarylike waves

One of the main properties of true solitary waves is that they preserve their shapes after collision [9,16]. It is interesting if the solitarylike waves described in the previous section behave in a similar way. To investigate collisions of solitarylike waves the 2 + 2 laminate with real material properties was impacted on both ends as shown in Fig. 15. The length was $L_c = 202$ mm. The impactor's thickness was $L_i = 6$ mm. They had velocities $V_a = 3500$ m/s and $V_b = 3200$ m/s

Figures 16(a) and 16(b) show both localized waves before collision at 60 mm from the impacted ends. It is clear that they have an almost symmetrical shape with small amplitude tails. The difference in their amplitudes is caused by the different velocities of impactors on corresponding ends.

Figure 17 corresponds to the depths 101 mm from both ends of the laminate with real properties where the two waves propagating in the opposite directions meet. The amplitude of the resulting pulse is increased as well as the amplitude of the tail; its duration was close to the durations of the pulses before collision.

Pulses after their collision are shown in Figs. 18(a) and 18(b) at distances 142 mm from the corresponding ends. We can see that after collision we have two localized waves with different amplitudes, which are smaller than the amplitudes before collision (Fig. 16), mostly because waves decay by traveling additional distances. It should be mentioned that the amplitudes of tails increased after collision due to dissipation.

Collisions of true solitary waves result in a phase shift [9,16]. To investigate if the phase shift is also characteristic for the collision of solitarylike waves, we compare two initially identical solitarylike waves created by the impact on the left end [shown in Fig. 16(a)], but traveling the same distance without collision. Figure 19(a) presents a comparison of the same wave traveling without collision and after a head-on collision at 122 mm from the left end. These two waves are superposed in Fig. 19(b) to demonstrate their similar profiles.

From Fig. 19(a) it is clear that a phase shift has occurred after collision, similar to the phase shift observed after collision

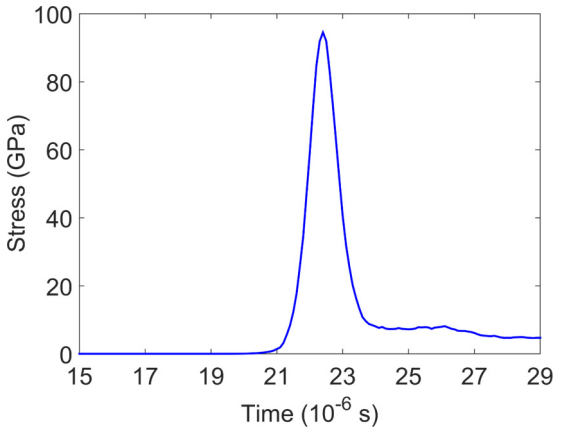

FIG. 17. (Color online) Resulting pulse due to collision of two waves propagating in the opposite direction at the middle of the laminate (at 101 mm depths from both ends).

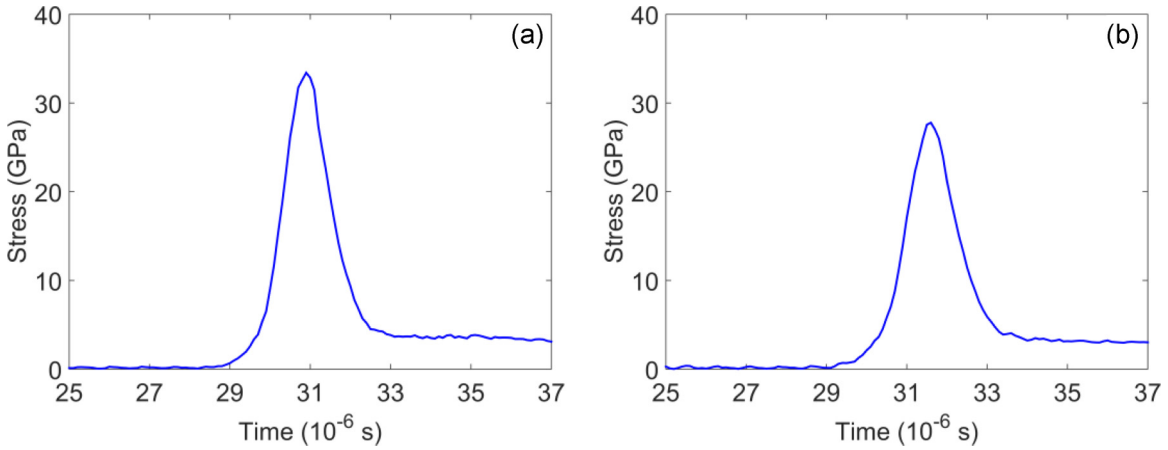

FIG. 18. (Color online) (a) Traveling wave at 142 mm depth from the left end of the laminate with real properties. (b) Traveling wave at 142 mm depth from the right end of the laminate. Both waves are shown after collision.

of true solitary waves. The two superposed waves in Fig. 19(b) demonstrate that they are very similar resembling the behavior of classic solitons, which completely reconstruct their shapes after collision. The difference between these solitarylike waves and true solitary waves is caused by the decay of the former due to the significant influence of dissipation at this level of stress.

IV. THEORETICAL APPROACH

The considered laminate material has a periodic structure and also exhibits significantly nonlinear behavior mostly due to nonlinearity in a constitutive equation. A combination of these properties supports the propagation of solitarylike waves under certain conditions of dynamic loading as observed numerically in the previous sections. The papers [16,17,20–22] introduce long wave approximation resulting in a Boussinesq-like wave equation to describe propagation of nondissipative solitarylike wave in laminates with relatively small dynamic elastic strains, about 10^{-2}. Nonlinearity in these papers was introduced based on nonlinear elasticity.

In this section we will combine dispersive and nonlinear properties of laminates incorporating them into a KdV-type equation, which supports solitary waves, and compare them with results of numerical calculations of a discrete system. Of course this approach, especially when it results in a stress pulse with dimensions comparable to the cell size of the laminate, needs verification by numerical calculations of a real discrete system. But if successful, it provides the scaling dependence of the parameters of a localized solitarylike stress pulse of high amplitude on physical and geometrical parameters of laminates.

The dispersion relation for laminated materials can be found in [29]; this expression considers the multiple reflections at the interfaces in the laminated material.

$$\cos(kd) = \cos\left(\frac{wd_a}{C_a}\right)\cos\left(\frac{wd_b}{C_b}\right) - \frac{1}{2}\left(\frac{Z_a}{Z_b} + \frac{Z_b}{Z_a}\right) \times \sin\left(\frac{wd_a}{C_a}\right)\sin\left(\frac{wd_b}{C_b}\right), \tag{11}$$

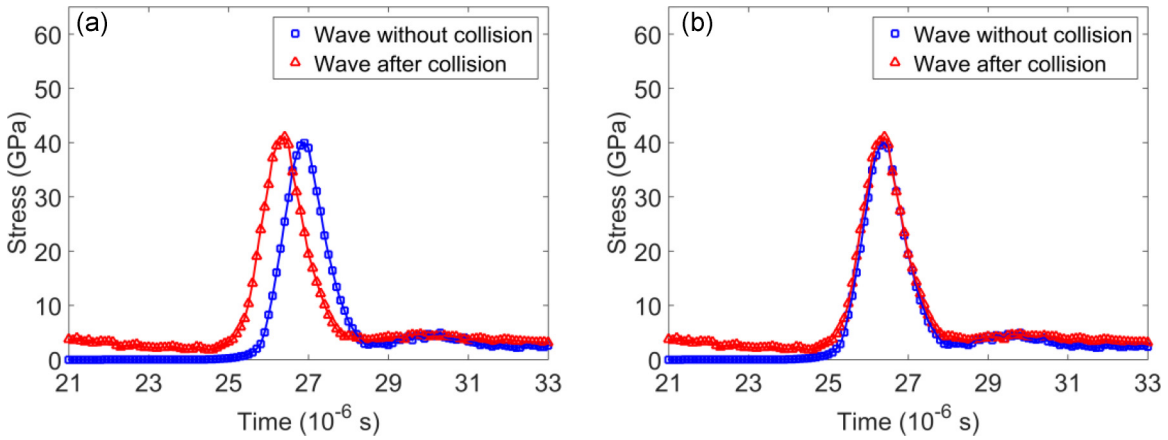

FIG. 19. (Color online) (a) The phase shift between two initially identical solitarylike waves created by the impact on the left end traveling the same distance of 122 mm without collision and after head-on collision; (b) the same waves are superposed to demonstrate their similar profiles.

where k is the wave number, w is wavelength, d_a and d_b are the respective sizes of each layer, cell size $d = d_a + d_b$, C_a and C_b refer to the respective sound speed in each layer, and Z_a and Z_b represent the respective impedances for each layer ($Z_i = \rho_i C_i$). In the limit of long wave approximation, $\lambda \gg d$, we get the following dispersion relation:

$$w^2 = \frac{k^2 d^2}{\left[\frac{d_a^2}{C_a^2} + \frac{d_b^2}{C_b^2} + \left(\frac{Z_a}{Z_b} + \frac{Z_b}{Z_a}\right)\left(\frac{d_a d_b}{C_a C_b}\right)\right]}\left[1 - \frac{k^2 d^2}{12}\right]$$
$$= C_0^2 k^2 \left(1 - \frac{k^2 d^2}{12}\right). \tag{12}$$

The first term in Eq. (12) provides an explicit expression for C_o for the laminate material, which is equivalent to the averaging approach presented in [16],

$$C_o^2 = \frac{d^2}{\frac{d_a^2}{C_a^2} + \frac{d_b^2}{C_b^2} + \left(\frac{Z_a}{Z_b} + \frac{Z_b}{Z_a}\right)\left(\frac{d_a d_b}{C_a C_b}\right)}. \tag{13}$$

In our numerical calculations, which included dissipation and more than one order of magnitude larger strains than in [16,17,20–22] (about 10^{-2}) we also observed solitarylike, slowly attenuating localized waves. But at these much higher strains it is more appropriate to introduce nonlinearity using the Hugoniot relation. Hugoniot parameters naturally reflect the nonlinear properties of materials because the shock wave is a typical example of the phenomena supported by a combination of nonlinear and dissipative properties. It should be mentioned that temperatures in solitarylike waves are smaller compared to shock temperatures at similar stress amplitudes, but because input of temperature to the stress at a given specific volume is relatively small, the use of the Hugoniot curve is appropriate. To introduce nonlinearity in the constitutive equation for each of the materials in the laminate we consider the Hugoniot curves [Eq. (14)] in stress versus strain coordinates for Al and W and their corresponding approximations using the second powers of strains [Eq. (18)]. The stress along the Hugoniot is defined as

$$P = \frac{C_o^2 (V_o - V)}{[V_o - s(V_o - V)]^2}, \tag{14}$$

where V_o and V correspond to the specific volume of the material at initial and deformed configuration, respectively, and s refers to the first coefficient of the Hugoniot curve on the $D-u$ plane (shock-particle velocity relation) which has the form

$$D = C_o + s\,u. \tag{15}$$

In this equation a single coefficient s is representing nonlinear behavior of the material in shock wave conditions. Strain in the shock wave in terms of specific volume can be written as

$$\epsilon = \frac{V_o - V}{V_o}. \tag{16}$$

By combining Eqs. (14) and (16) we obtain the Hugoniot stress-strain relation

$$P = \frac{C_o^2}{V_o}\left[\frac{\epsilon}{(1 - s\,\epsilon)^2}\right]. \tag{17}$$

At relatively low values of strains (below 0.15 for Al and 0.1 for W) we can approximate the behavior of Al and W using the following equation with corresponding coefficients:

$$P = \frac{C_o^2}{V_o}[\epsilon(1 + 2s\,\epsilon)]. \tag{18}$$

The Hugoniot curves and their approximations by Eq. (18) are presented in Figs. 20(a) and 20(b). For comparison, zero Kelvin compression curves, isentrope (Al [30], W estimated from [34]), and curves based on third order elastic constants are also presented. The latter ones are described by the following equation:

$$\sigma = \gamma\epsilon + \frac{\beta}{2}\epsilon^2, \tag{19}$$

where coefficients γ and β are defined by

$$\gamma = \lambda + 2\mu, \tag{20}$$

$$\beta = 3(\lambda + 2\mu) + 2(A + 3B + C), \tag{21}$$

where λ and μ are the Lamé parameters and A, B, and C are the third order elastic constants [35].

It is clear that using third order elastic constants in our range of stresses is not adequate. At the same time deviation of

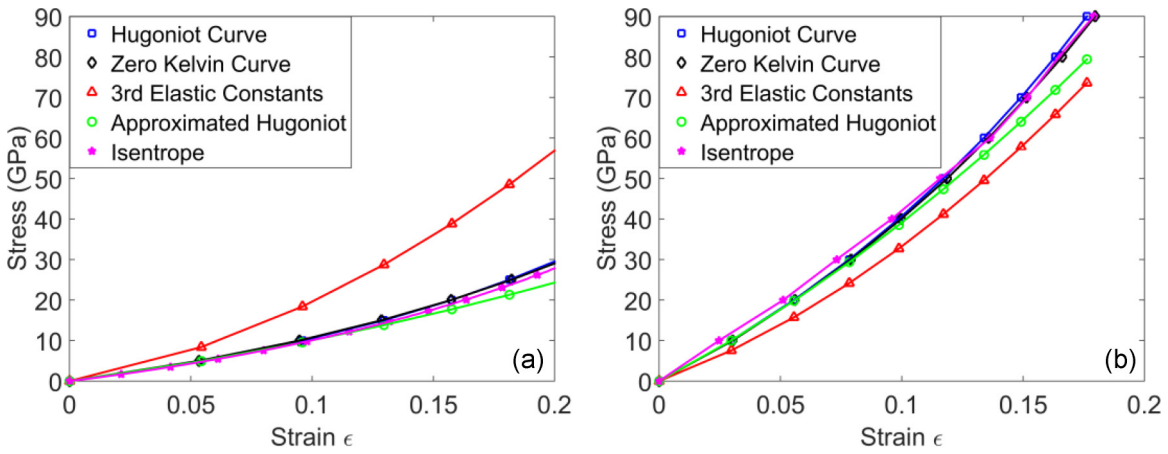

FIG. 20. (Color online) Nonlinear stress-strain relations for Al (a), and W (b) based on Hugoniot curves, static compression based on third order elastic constants, zero Kelvin curves, isotherm and approximation of Hugoniot curves using terms only with second power law of strains, Eq (16).

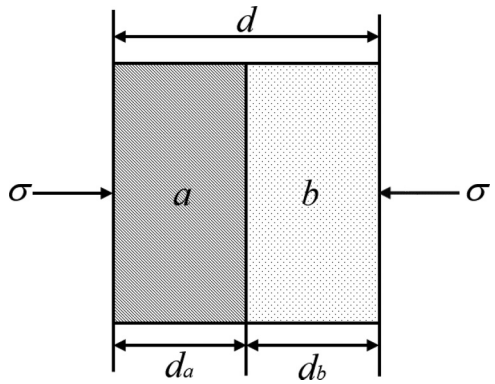

FIG. 21. Single cell with unit area made of material a and b.

stresses on the Hugoniot curve from the values corresponding to zero Kelvin curve at the same strains are within a few percent for Al and W at stresses below 40 GPa (strains below 0.25 for Al and below 0.1 for W). Thus we can use the Hugoniot curves approximated by Eq. (18) as a reasonable representation of isentropic behavior. It is appropriate taking into account that on the steady state of the propagation of localized stress pulses materials experience isentropic compression paths, which are between the zero Kelvin curve and Hugoniot states. It should be emphasized that we are looking for a nondissipative description of the single stress pulse despite existing dissipation at this level of stress. Results of numerical calculations presented above demonstrate that dissipation, resulting in the pulse attenuation, does not change the nature of the pulse coming from a balance of nonlinearity and dispersion similar to the case of strongly nonlinear solitary waves in granular lattices [9].

To find the nonlinearity coefficient in the stress-strain relation for the laminate material we consider its single cell with unit area as depicted in Fig. 21.

We need to find constants K_{eq}, α_{eq} describing the behavior of the unit cell under compression with effective total strain ε_t. We define the total strain of the deformed cell as

$$\begin{aligned}\epsilon_t &= \frac{(d_{\mathrm{Al}} + d_{\mathrm{W}}) - \left(d_{\mathrm{Al}_o} + d_{\mathrm{W}_o}\right)}{d_{\mathrm{Al}_o} + d_{\mathrm{W}_o}} \\ &= \frac{d_{\mathrm{Al}} - d_{\mathrm{Al}_o}}{d_{\mathrm{Al}_o} + d_{\mathrm{W}_o}} + \frac{d_{\mathrm{W}} - d_{\mathrm{W}_o}}{d_{\mathrm{Al}_o} + d_{\mathrm{W}_o}} \\ &= \epsilon_a\left(\frac{d_{\mathrm{Al}_o}}{d_{\mathrm{Al}_o} + d_{\mathrm{W}_o}}\right) + \epsilon_{\mathrm{b}}\left(\frac{d_{\mathrm{W}_o}}{d_{\mathrm{Al}_o} + d_{\mathrm{W}_o}}\right) \\ &= \epsilon_{\mathrm{Al}}\,\tau + \epsilon_{\mathrm{W}}(1-\tau), \end{aligned} \tag{22}$$

where d_{Al_o}, d_{W_o} represent the original length of Al, W; the symbols d_{Al}, d_{W} are related to a deformed cell. For the system being in equilibrium, $\sigma_{\mathrm{Al}} = \sigma_{\mathrm{W}} = \sigma$, where σ is the stress applied to the cell. The equation for a total strain including a nonlinear term quadratic with respect to ϵ^2 is represented by the following expression:

$$\sigma \approx \frac{K_{\mathrm{Al}}K_{\mathrm{W}}}{(1-\tau)K_{\mathrm{Al}} + \tau K_{\mathrm{W}}}\epsilon + \frac{\left[\tau K_{\mathrm{W}}^3\alpha_{\mathrm{Al}} + (1-\tau)K_{\mathrm{Al}}^3\alpha_{\mathrm{W}}\right]}{\left[(1-\tau)K_{\mathrm{Al}} + \tau K_{\mathrm{W}}\right]^3}\epsilon^2, \tag{23}$$

This gives us the expressions for coefficient of nonlinearity α_{eq} and linear elastic modulus K_{eq} representing the global response of the cell,

$$\alpha_{eq} = \frac{\left[\tau K_{\mathrm{W}}^3\alpha_{\mathrm{Al}} + (1-\tau)K_{\mathrm{Al}}^3\alpha_{\mathrm{W}}\right]}{\left[(1-\tau)K_{\mathrm{Al}} + \tau K_{\mathrm{W}}\right]^3}, \tag{24}$$

$$K_{eq} = \frac{\mathrm{K_{Al}K_W}}{(1-\tau)\mathrm{K_{Al}} + \tau\mathrm{K_W}}. \tag{25}$$

Apparently that coefficient of nonlinearity is the same for laminates with the same volume of components. The wave equation, being a long wave approximation of a discrete, nondissipative system and having the same dispersive relation and reflecting nonlinear behavior, is the Boussinesq equation

$$U_{tt} = C_o^2 U_x + \beta U_{xxxx} - \psi U_x U_{xx}, \tag{26}$$

where coefficients β and ψ are related to materials parameters in the following way:

$$\beta = \frac{d^2 C_o^2}{12}. \tag{27}$$

Unlike the coefficient of nonlinearity and sound speed which is the same for laminates with the same volume ratio of components, the coefficient of dispersion depends on the characteristic scale of laminate d. Parameter ψ is the coefficient related to the nonlinear part of the force applied to the cell composed from the elements of the discrete system,

$$\psi = \frac{2\alpha_{eq}C_o^2}{K_{eq}}. \tag{28}$$

This equation can be converted to a KdV equation in the same approximation:

$$\zeta_t + C_o\zeta_x + S\zeta_{xxx} + \nu\zeta\zeta_x = 0, \tag{29}$$

$$S = \frac{\beta}{2}, \tag{30}$$

$$\nu = \frac{\psi}{2C_o}. \tag{31}$$

The KdV equation has a solitary wave solution of the form

$$\zeta = \zeta_m\,\mathrm{sech}^2\left[\left(\frac{\psi\zeta_m}{12\beta}\right)^{\frac{1}{2}}(x - vt)\right]. \tag{32}$$

The equation for the full width at half maximum (FWHM) of this pulse (w) expressed in terms of the cell size, thicknesses of layers, and linear and nonlinear properties of components as well as an amplitude of stress pulse is presented below:

$$\mathrm{FWHM} = \frac{1.76dK_{eq}^{1/2}}{\left(2\alpha_{eq}\ \zeta_m\right)^{1/2}}. \tag{33}$$

It is interesting that though the FWHM of the pulse in laminate w is scaled linearly with the cell size d the individual thicknesses of layers are also affecting the size of the solitary wave present in the values of K_{eq} and α_{eq}. It means that laminates with the same cell size d will have different values of w if the thicknesses of individual layers are different.

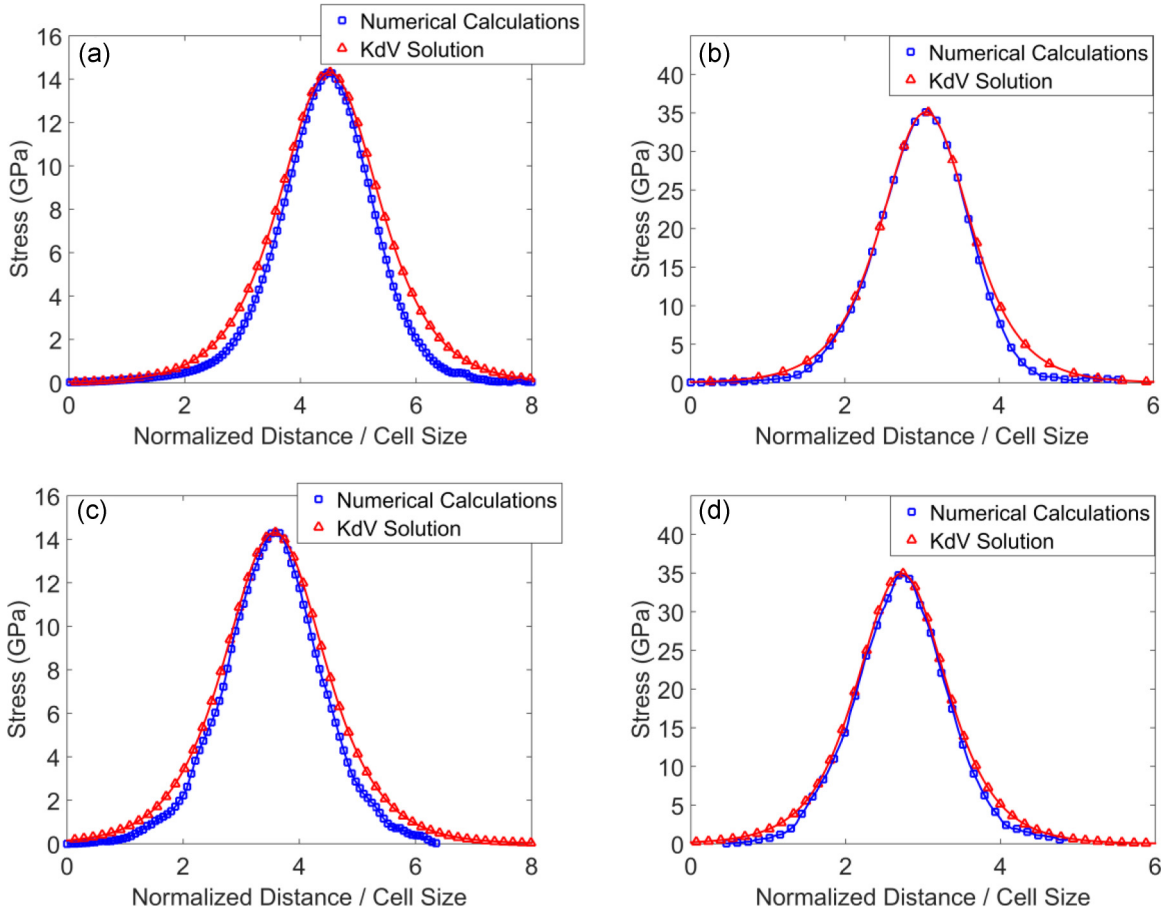

FIG. 22. (Color online) Comparison of KdV solitary solution with nonlinearity parameters taken from Hugoniot curve [Eq. (18)] to the shapes of solitarylike waves found on numerical simulations: (a) The wave in numerical simulation corresponding to the depth of 72 mm in the $2+2$ laminate with artificially small $Y_{\max}$ laminate impacted by a 2-mm Al plate with a velocity of 2800 m/s. (b) The wave in numerical simulation corresponding to the depth of 32 mm in the $1+1$ laminate with artificially small $Y_{\max}$ impacted by a 2-mm Al plate with a velocity of 2800 m/s. (c,d) comparison of waves in corresponding laminates ($2+2$ and $1+1$) with real properties.

The speed of the solitary wave is given by

$$V = C_o + \frac{\nu}{3}\zeta_m, \tag{34}$$

$$\nu = \frac{\psi}{2C_o} = \frac{2dC_{\mathrm{Al}}^2\rho_{\mathrm{Al}}C_{\mathrm{W}}^2\rho_{\mathrm{W}}\left(C_{\mathrm{Al}}^6\rho_{\mathrm{Al}}^3K_{\mathrm{W}}S_{\mathrm{W}}d_{\mathrm{W}} + C_{\mathrm{W}}^6\rho_{\mathrm{W}}^3K_{\mathrm{Al}}S_{\mathrm{Al}}d_{\mathrm{Al}}\right)}{K_{\mathrm{Al}}K_{\mathrm{W}}\left(C_{\mathrm{Al}}^2\rho_{\mathrm{Al}}d_{\mathrm{W}} + C_{\mathrm{W}}^2\rho_{\mathrm{W}}d_{\mathrm{Al}}\right)(\rho_{\mathrm{Al}}d_{\mathrm{Al}} + d_{\mathrm{W}}\rho_{\mathrm{W}})}. \tag{35}$$

Now we explore if this approximation satisfactorily describes the shape of solitarylike stress pulses and their speeds observed in numerical calculations.

Figures 22(a)–22(d) present the shapes of stress pulse found in LS-DYNA numerical simulations and KdV solitary wave solution [Eq. (32)] for maximum stresses below 35 GPa where cold curve and isentropic compression are very well approximated by nonlinear equation (18). The pulse shapes generated in the numerical calculations performed with real material properties as well as the one with artificially small $Y_{\max}$ are shown in Fig. 22.

We can see that space scales and shapes of stress pulses observed in numerical calculations are satisfactory described by long wave KdV solitary wave solution despite the characteristic width of the pulse being close to the cell size and dissipation present in numerical calculations. It should be mentioned that the full width at half maximum (FWHM) for these pulses is only about two cells. The pulse in numerical calculation is narrower than KdV solution, and the FWHM of the KdV solitary wave solution is about 12% larger than the corresponding pulse width in numerical calculations in the case of a solitarylike wave in a $2+2$ laminate [Fig. 22(c)].

It is interesting to check if a presented solitary wave solution is also a reasonable approximation for a broader range of wave amplitudes, specifically for significantly larger stresses where nonlinear behavior deviates more significantly from

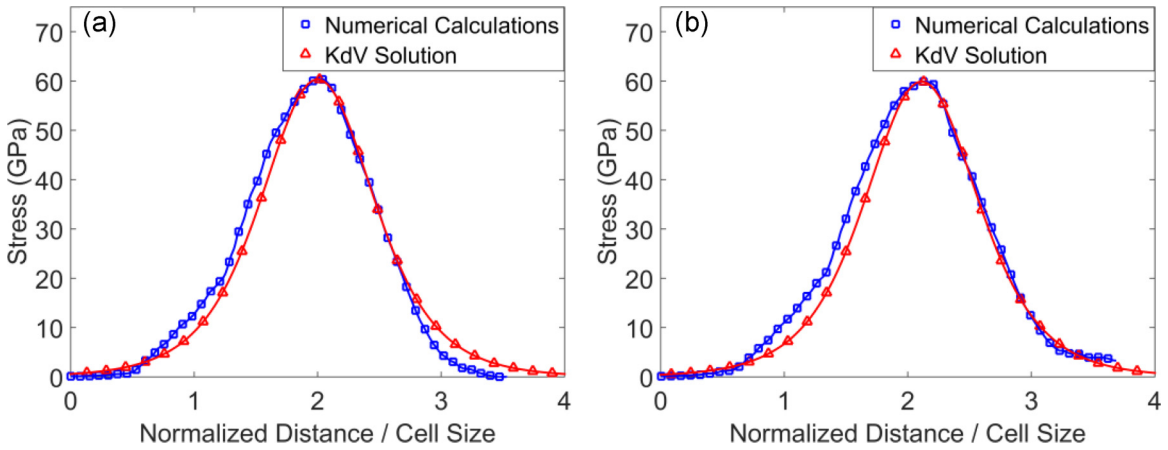

FIG. 23. (Color online) Comparison of KdV solitary solution with nonlinearity parameters taken from an approximated Hugoniot curve [Eq. (16)] to the wave found on numerical simulations. The wave in the numerical simulation corresponds to the depth of 132 mm in a $2+2$ laminate impacted by an 8-mm Al plate with a velocity of 2800 m/s and artificially small $Y_{\max}$ (a) and in laminate with real material properties (b).

the approximation described by Eq. (18). The corresponding shape of the stress pulse at these stresses is shown in Fig. 23.

The value of FWHM in this case is about one cell size only. It is amazing that the KdV solitary wave, obtained as a solution of a wave equation being a weakly nonlinear and long wave approximation of a discrete system, is still a satisfactory approximation for the shape of the very short localized pulse observed in numerical calculations. Thus Eq. (33) provides a correct scaling of the size of solitarylike pulses and a reasonable description of their shapes in a very broad range of stress amplitudes.

Another property of KdV solitary waves is a linear dependence of their speed on the stress amplitude [Eq. (34)]. Figure 24 presents a comparison of the dependence of the speed of pulses on the stress amplitude found in numerical calculations for laminates with different cell sizes with a similar dependence for KdV solitary waves [Eq. (34)].

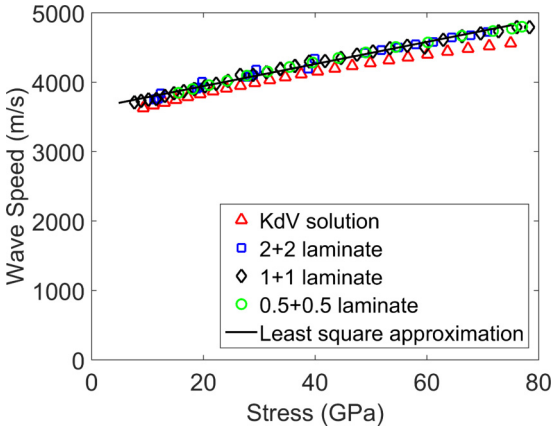

FIG. 24. (Color online) Dependence of the speed of the localized wave in Al-W $2+2$, $1+1$, and $0.5+0.5$ laminates found in numerical calculations on maximum stress (on the interface between Al and W) and corresponding to Eq. (34) for the speed of a KdV solitary wave.

It is clear that the linear relationship between the speed of the pulse and maximum stress found for the KdV solitary wave is a satisfactory approximation in the whole investigated range of stress amplitudes for different laminates. It is important that the speed of the solitarylike wave in numerical calculations is not dependent on the cell size, as can be expected from the proposed analogy with the KdV soliton. It is interesting that at the same cell size, but at different individual thicknesses of layers (determining the relative volume of components) the speed of a solitarylike wave will be different. This dependence is represented by values of K_{eq} and α_{eq} depending on the volume fraction of the components. It means that laminates with the same cell size d will have different values of the slope of the speed versus stress amplitude if the thicknesses of individual layers are different.

It should be mentioned that sound speed for the laminate, based on Eq. (13), is $C_{eq} = 3381$ m/s. From the graph presented in Fig. 24 we can see that the speed of the solitary wave in the KdV approximation and also in numerical calculations is larger than the sound speed in the laminate in a long wave approximation; thus this pulse is supersonic with respect to the long wave sound speed in the laminate. However, its speed in the investigated range of stresses is smaller than the sound speed in Al, and at maximum stresses below 30 GPa is also smaller than in W. As a result short wave length disturbances with the space scale compared to the thickness of the layers can escape into the area in front of the propagating pulse leaking the energy from the pulse and contributing to the amplitude attenuation. This mechanism is additional to the dissipation and presents another reason that these propagating pulses are not truly solitary waves despite being satisfactorily described by the KdV soliton solution. This mechanism also contributes to the nonelastic collision of these localized pulses.

V. CONCLUSIONS

The existence of solitarylike localized waves in laminate material Al-W in a broad range of stress amplitude (10–80 GPa) was demonstrated using numerical calculations.

It was shown that the dissipation due to viscoplastic behavior causes significant decay of amplitude of these solitarylike stress pulses, but their space scale and shape are closely approximated by KdV solution.

These solitarylike waves exhibit behavior similar to classical KdV solitons, e.g., a dependence of speed and width on the stress amplitude. The different durations of incoming pulse, with respect to characteristic time scale of the laminate, result in either the formation of only one localized solitarylike wave, a train of such waves, or in an oscillatory shock–like wave. It has also been shown that interaction between these waves results in a phase shift, which is similar to behavior in classic solitons, although it also shows a nonelastic behavior.

A theoretical framework based on a weekly nonlinear KdV equation supporting a solitary wave was presented. To introduce a nonlinearity parameter, readily available shock Hugoniot data were used together with the exact dispersion relation for a linear elastic laminate. The shape and speed of the localized waves found in numerical calculations are in satisfactory agreement with the KdV solitary wave in a broad range of stress amplitudes.

This approach allowed us to arrive at the analytic equation for width and speed of the observed solitarylike stress pulses using nonlinear properties of components and geometry of laminate. It allows the design of layered materials for optimal protection, e.g., to prevent spall, and to understand the nature of pulses propagating under extremely short pulse loading, e.g., produced by powerful lasers.

ACKNOWLEDGMENTS

P.F.N. wants to thank CONACYT – UC-MEXUS for providing the funding that made this work possible.

[1] R. Kinslow, *High-Velocity Impact Phenomena* (Elsevier, New York, 2012).
[2] S. P. Marsh, *LASL Shock Hugoniot Data*, Vol. 5 (University of California Press, Berkeley, 1980).
[3] R. McQueen, S. Marsh, and J. Fritz, Hugoniot equation of state of twelve rocks, J. Geophys. Res. **72**, 4999 (1967).
[4] S. M. Rytov, Acoustical properties of a thinly laminated medium, Sov. Phys. Acoust. **2**, 68 (1956).
[5] C.-T. Sun, J. D. Achenbach, and G. Herrmann, Continuum theory for a laminated medium, J. Appl. Mech. **35**, 467 (1968).
[6] H. J. Sutherland and R. Lingle, Geometric dispersion of acoustic waves by a fibrous composite, J. Compos. Mater. **6**, 490 (1972).
[7] D. Drumheller and H. Sutherland, A lattice model for stress wave propagation in composite materials, J. Appl. Mech. **40**, 149 (1973).
[8] R. Hofmann, D. J. Andrews, and D. Maxwell, Computed shock response of porous aluminum, J. Appl. Phys. **39**, 4555 (1968).
[9] V. F. Nesterenko, *Dynamics of Heterogeneous Materials* (Springer Science & Business Media, New York, 2001).
[10] C. Wei, B. Maddox, A. Stover, T. Weihs, V. Nesterenko, and M. Meyers, Reaction in Ni-Al laminates by laser-shock compression and spalling, Acta Mater. **59**, 5276 (2011).
[11] C. Wei, V. Nesterenko, T. Weihs, B. Remington, H.-S. Park, and M. Meyers, Response of Ni/Al laminates to laser-driven compression, Acta Mater. **60**, 3929 (2012).
[12] V. Nesterenko, V. Fomin, and P. Cheskidov, Damping of strong shocks in laminar materials, J. Appl. Mech. Tech. Phys. **24**, 567 (1983).
[13] V. Nesterenko, V. Fomin, and P. Cheskidov, Attenuation of strong shock waves in laminar materials, *Nonlinear Deformation Waves* (Springer-Verlag, Berlin, 1983), p. 191.
[14] D. Benson and V. Nesterenko, Anomalous decay of shock impulses in laminated composites, J. Appl. Phys. **89**, 3622 (2001).
[15] N. K. Akhmadeev and R. K. Bolotnova, Propagation of stress waves in layered media under impact loading (acoustical approximation), J. Appl. Mech. Tech. Phys. **26**, 114 (1985).
[16] D. H. Yong and R. J. LeVeque, Solitary waves in layered nonlinear media, SIAM J Appl. Math. **63**, 1539 (2003).
[17] J. Engelbrecht, A. Berezovski, and A. Salupere, Nonlinear deformation waves in solids and dispersion, Wave Motion **44**, 493 (2007).
[18] R. D. Mindlin, Micro-structure in linear elasticity, Arch. Ration. Mech. Anal. **16**, 51 (1964).
[19] S. Zhuang, G. Ravichandran, and D. E. Grady, An experimental investigation of shock wave propagation in periodically layered composites, J. Mech. Phys. Solids **51**, 245 (2003).
[20] A. Salupere, K. Tamm, and J. Engelbrecht, Numerical simulation of interaction of solitary deformation waves in microstructured solids, Int. J. Non-Linear Mech. **43**, 201 (2008).
[21] J. Engelbrecht, A. Salupere, and K. Tamm, Waves in microstructured solids and the boussinesq paradigm, Wave Motion **48**, 717 (2011).
[22] I. V. Andrianov, V. V. Danishevskyy, O. I. Ryzhkov, and D. Weichert, Numerical study of formation of solitary strain waves in a nonlinear elastic layered composite material, Wave Motion **51**, 405 (2014).
[23] J. O. Hallquist, *LS-DYNA Theory Manual* (Livermore Software Technology Corporation, Livermore, CA, 2006); http://www.lstc.com/pdf/ls-dyna_theory_manual_2006.pdf.
[24] D. Steinberg, S. Cochran, and M. Guinan, A constitutive model for metals applicable at high-strain rate, J. Appl. Phys. **51**, 1498 (1980).
[25] D. Steinberg, *Equation of State and Strength Properties of Selected Materials* (Lawrence Livermore National Laboratory, Livermore, CA, 1996).
[26] L. C. Chhabildas and J. R. Asay, Rise-time measurements of shock transitions in aluminum, copper and steel, J. Appl. Phys. **50**, 2749 (1979).
[27] J. C. Crowhurst, M. R. Armstrong, K. B. Knight, J. M. Zaug, and E. M. Behymer, Invariance of the Dissipative Action at Ultrahigh Strain Rates Above the Strong Shock Threshold, Phys. Rev. Lett. **107**, 144302 (2011).
[28] J. Asay, L. Chhabildas, and D. Dandekar, Shear strength of shock-loaded polycrystalline tungsten, J. Appl. Phys. **51**, 4774 (1980).

[29] E. Lee and W. H. Yang, On waves in composite materials with periodic structure, SIAM J. Appl. Math. **25**, 492 (1973).

[30] G. Kerley, Theoretical equation of state for aluminum, Int. J. Impact Eng. **5**, 441 (1987).

[31] A. Rosas, A. H. Romero, V. F. Nesterenko, and K. Lindenberg, Observation of Two-Wave Structure in Strongly Nonlinear Dissipative Granular Chains, Phys. Rev. Lett. **98**, 164301 (2007).

[32] A. Rosas, A. H. Romero, V. F. Nesterenko, and K. Lindenberg, Short-pulse dynamics in strongly nonlinear dissipative granular chains, Phys. Rev. E **78**, 051303 (2008).

[33] E. B. Herbold and V. F. Nesterenko, Shock wave structure in a strongly nonlinear lattice with viscous dissipation, Phys. Rev. E **75**, 021304 (2007).

[34] L. Chhabildas, J. Asay, and L. Barker, Dynamic quasi-isentropic loading of tungsten, High Press. Sci. Technol. **5**, 842 (1990).

[35] C. Cattani and Rushchitskii, *Wavelet and Wave Analysis as Applied to Materials with Micro or Nanostructure*, Series on Advances in Mathematics for Applied Sciences (World Scientific, Hackensack, NJ, 2007).